JOURNAL OF MOLECULAR SPECTROSCOPY 120, 381–402 (1986)

Fourier Transform Spectroscopy of the $A^3\Pi$–$X^3\Sigma^-$ Transition of NH

C. R. BRAZIER, R. S. RAM, AND P. F. BERNATH

Department of Chemistry, University of Arizona, Tucson, Arizona 85721

The $A^3\Pi$–$X^3\Sigma^-$ transition of NH has been observed using a high-resolution Fourier transform spectrometer. The first three vibrational levels in each state were observed and the vibrational, fine structure, and rotational constants obtained.

I. INTRODUCTION

The $A^3\Pi$–$X^3\Sigma^-$ system of NH has been known for a very long time. The bands were first described by Eder (*1*) in 1893 and have been the subject of many subsequent investigations. The main branches of the 0–0 and 1–1 bands were assigned from emission spectra by Funke (*2*) in the 1930s. The analysis was greatly improved by the observation of the 1–0 and 0–0 bands in absorption by Dixon (*3*). His use of a room temperature source made it possible to observe most of the satellite branches, which drop rapidly in intensity with increasing rotation. Dixon was thus able to correctly assign his measurements together with those of Funke, and obtained reasonably accurate rotational and fine structure constants for the ground and excited states.

Additional measurements on the 0–0 and 1–1 bands were made by Murai and Shimauchi (*4*) while the weak 0–1, 1–2, 1–0, and 2–1 bands were recorded by Malicet *et al.* (*5*). The $A^3\Pi$–$X^3\Sigma^-$ system of the isotopic species ND has been studied by Shimauchi (*6*) and by Bollmark *et al.* (*7*).

The accuracy of all these measurements was limited to, at best, ± 0.03 cm^{-1} by the use of grating spectrographs. The development of CW dye lasers around 1970 did not help as the transition occurs near 3360 Å—well into the ultraviolet. However, the recent development of intracavity frequency doubling has made it possible to record laser-induced fluorescence spectra in the UV. Ubachs *et al.* (*8*) recorded the laser-induced fluorescence spectrum of the $A^3\Pi$–$X^3\Sigma^-$ system of NH in a molecular beam. Their linewidth was sufficiently reduced that they were able to resolve the hyperfine structure of both nuclei. While they were able to measure hyperfine splittings accurate to ± 0.00007 cm^{-1}, they did not attempt an absolute frequency calibration of the rotational lines and hence did not determine any rotational or fine structure constants.

We have remeasured the $A^3\Pi$–$X^3\Sigma^-$ system of NH using a Fourier transform spectrometer with a precision of ± 0.0002 cm^{-1} for the strong, unblended lines in the 0–0 band, an improvement of more than two orders of magnitude over the previous best measurements.

Several high-resolution studies of the ground state have been made, measuring both pure rotation and vibration–rotation transitions. The far-infrared laser magnetic resonance spectrum was recorded by Radford and Litvak (*9*) and by Wayne and Radford

0022-2852/86 $3.00

(*10*). With the development of tunable infrared lasers additional experiments became possible. Van der Heuval *et al.* (*11*) recorded the zero field pure rotational spectrum in the far infrared, while Bernath and Amano (*12*) observed the vibrational fundamental in the infrared. The infrared fundamental was observed by matrix isolation spectroscopy by Milligan and Jacox (*13*). Several vibration–rotation bands have been observed by Fourier transform emission spectroscopy at moderate resolution (*14, 15*) and, recently, at high resolution (*16, 17*).

There are four known singlet states of NH, $a^1\Delta$, $b^1\Sigma^+$, $c^1\Pi$, and $d^1\Sigma^+$. All four allowed transitions between these states have been studied. The c–a system at 3240 Å, just to the blue of the triplet system, has been extensively analyzed. The papers by Pearse (*18*), Dieke and Blue (*19*), and Nakamura and Shidei (*20*) in the 1930s all identified this system at about the same time and gave comparable results. More recently this system was recorded at higher precision by Cheung *et al.* (*21*) and by Ramsay and Sarre (*22*). The $c^1\Pi$–$a^1\Delta$ transition was also observed in our Fourier transform spectrum. The higher precision of these measurements made possible the determination of the Λ-doubling interaction in the $a^1\Delta$ state. Dymanus has also determined the Λ doubling in $a^1\Delta$ by the high-resolution laser-induced fluorescence experiment in a molecular beam (*23*). Our data on this system will be published elsewhere (*24*).

The $c^1\Pi$–$b^1\Sigma^+$ system at 4502 Å has been studied by Lunt *et al.* (*25*) and by Whittaker (*26*). The $d^1\Sigma^+$–$c^1\Pi$ transition at 2530 Å is also well known and has been studied by Lunt *et al.* (*27*), Whittaker (*28*), and Krishnamurty and Narasimham (*29*). The other allowed transition $d^1\Sigma^+$–$b^1\Sigma^+$ is in the vacuum UV at 1620 Å and has been observed by Graham and Lew (*30*). The $a^1\Delta$ vibrational fundamental of NH has been studied by Hall *et al.* (*31*) by color center laser kinetic spectroscopy. Very recently Leopold *et al.* (*32*) observed the far-infrared laser magnetic resonance spectrum of the $a^1\Delta$ state of NH and ND.

An important advance in the spectroscopy of NH came with the observation of the $b^1\Sigma^+$–$X^3\Sigma^-$ intercombination band by Masanet *et al.* (*33*). From this emission the location of the lowest singlet $a^1\Delta$ could be determined relative to the ground state. The singlet–triplet splitting was also determined by photoelectron spectroscopy of NH^- by Engelking and Lineberger (*34*). The electron affinity of NH was established to be 0.381 eV in this photoelectron experiment. More recently high-resolution observations of the $b^1\Sigma^+$–$X^3\Sigma^-$ system have been made (*35*) as well as detection of $a^1\Delta$–$X^3\Sigma^-$ emission (*36*). The b–X measurements of Cossart (*35*) result in a singlet–triplet splitting of 12 688.39(10) cm^{-1} for $a^1\Delta$ ($v = 0$, $J = 2$) − $X^3\Sigma^-$ ($v = 0$, $J = 1$, $N = 0$) using the line positions of Refs. (*24, 26, 35*).

There have been many photochemical studies involving NH (*37–45*) produced by laser photolysis. Using precursors such as ammonia, hydrazine, and hydrazoic acid, the internal energy distributions, radiative lifetimes, and quenching rates for the different states of NH initially populated have been determined. Similar results have also been obtained using electron impact dissociation (*46*). Cooling of spin–orbit components and population inversion in the $A^3\Pi$ state has been observed by Carrick and Engelking in a corona excited nozzle expansion (*47*).

The transition probabilities for several bands of NH have been determined. Lents (*48*) published a review of the molecular constants for all the known states of NH.

The absolute absorption intensities were determined by Harrington *et al.* (*49*) in a shock tube. The lifetime of the $A^3\Pi$–$X^3\Sigma^-$ system has recently been remeasured by Fairchild *et al.* (*50*) for several vibrational bands. They comment that the Franck-Condon factors computed from RKR potential curves are not very accurate because of the poor quality of the spectroscopic constants for the higher vibrational levels. We hope the new constants determined in this work will make these calculations more accurate. This group has also recently measured quenching rate constants for the $A^3\Pi$ state (*51*).

Smith *et al.* (*52*) studied the variation of lifetimes with rotation and vibration for both the $A^3\Pi$ and $c^1\Pi$ states. They discovered predissociations in both states, caused by crossing of a repulsive $^5\Sigma^-$ state. The observed intensities in the bands which we have studied are consistent with their results. The observation of rotational predissociation by Graham and Lew (*30*) and Zetzsch (*53*) has resulted in an accurate determination of the dissociation energy $D_0^0 = 3.46 \pm 0.01$ eV. Foner and Hudson (*54*) have measured the ionization potential by mass spectroscopy to be 13.47 ± 0.05 eV. The dipole moment has been measured by Scarl and Dalby (*55*) to be 1.38 D in the ground state using the high field Stark effect, where the electric discharge which produces the molecules also provides the Stark field. The standard heat of formation of NH is 85.2 ± 0.4 kcal/mole (*56*).

All of these experimental results can be compared with those obtained from theoretical calculations by, for example, Kouba and Öhrn (*57*), Hay and Dunning (*58*), and Meyer and Rosmus (*59*).

The frequent observation of NH in flames and other energetic environments has resulted in much interest in the spectrum. The species NH_i have significant effects on the production of NO_x in fuel–air combustion (*60, 61*). The $A^3\Pi$–$X^3\Sigma^-$ transition can be used to monitor the concentration of NH in flames (*62, 63*).

NH was first observed in a nonlaboratory source by Fowler and Gregory (*64*), in the spectrum of the sun, although at that time (1918) the 3360-Å band was incorrectly assigned to ammonia. Since then NH has been found in stellar atmospheres (*65, 66*) and in comets (*67, 68*) by the spectroscopic observation of the $A^3\Pi$–$X^3\Sigma^-$ transition. With the current interest in infrared astronomy, the vibration–rotation spectrum of NH has also been observed in stellar atmospheres by Fourier transform spectroscopy (*69, 70*).

II. EXPERIMENTAL DETAILS

NH molecules were produced in a standard copper hollow cathode discharge, operated at a current of 430 mA with a continuous flow of 4.5 Torr of He. Small amounts of nitrogen and hydrogen,40 and 120 mTorr, respectively, were added. These parameters were adjusted to optimize the production of NH. The emission spectrum was recorded through a copper sulfate filter with the Fourier transform spectrometer associated with the McMath Solar Telescope of the National Solar Observatory[1] at Kitt Peak. A total of 15 scans were coadded in one hour of observation. The unapodized instrumental resolution was 0.042 cm^{-1}.

[1] The National Solar Observatory is operated by the Association of Universities for Research in Astronomy, Inc., under contract with the National Science Foundation.

The signal-to-noise ratio for the strong lines of the 0–0 band was more than 1000 to 1. The 1–1 band was almost as strong at about 500 to 1 while the other observed bands 2–2, 0–1, 1–2, 1–0, and 2–1 were all much weaker. A sample of the *P*-branch region of the $\Delta v = 0$ sequence is shown in Fig. 1. The linewidth varied to some extent with rotational and vibrational quantum number but was typically 0.18–0.2 cm^{-1} for the strong 0–0 lines. As a result the relative line positions could be determined to a precision of 0.0002 cm^{-1} (the linewidth divided by the signal-to-noise ratio) for strong unblended lines. The accuracy of the measurements is less than this and is limited by the absolute wavelength calibration. This was rather difficult to achieve as only a few He(I) and He(II) lines were observed with high signal-to-noise, and these had not previously been measured with very high accuracy.

Only one He line, 4^1P–2^1S, proved suitable for calibration because of a symmetric lineshape and a signal-to-noise ratio greater than 500. The previous measurement 25 215.270 ± 0.005 cm^{-1} for this transition (*71*) was improved by comparing a He/Ti hollow cathode emission spectrum with an Ar/Ti hollow cathode emission spectrum. Norlen (*72*) has made excellent line-position measurements for argon. Titanium atomic lines were used as a transfer standard to give 25 215.2824 ± 0.003 cm^{-1} for He 4^1P–2^1S. The estimated error of ±0.003 cm^{-1} means that our absolute accuracy is still a factor of 10 larger than the precision of the strong lines. Any improvement in the accuracy of the He 4^1P–2^1S line measurement or a direct measurement of a strong NH transition by laser methods would bring the estimated accuracy of our work closer to the precision.

III. ANALYSIS

The interferogram was transformed by standard methods to yield the spectrum, which covered the range from 23 800 to 35 600 cm^{-1}. This range covers the $\Delta v = 0$

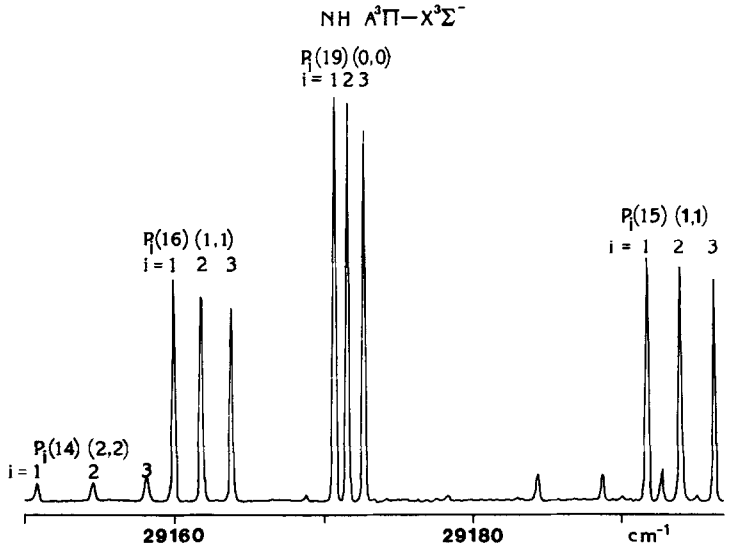

FIG. 1. A segment of the NH $A^3\Pi-X^3\Sigma^-$ spectrum in the *P*-branch region. Tripled rotational lines of the 0–0, 1–1 and 2–2 vibrational bands are labeled with N''.

and $\Delta v = \pm 1$ vibrational bands of the $A^3\Pi$–$X^3\Sigma^-$ system of NH. In addition, it covers the $c^1\Pi$–$a^1\Delta$ system, and our analysis of this system will be reported elsewhere (*24*). Some problems were experienced with bands of N_2 and N_2^+ which occur throughout the region. There were many areas with strong bands due to N_2 and N_2^+ but generally these did not overlap the NH lines. There was also a weak background throughout much of the region of interest which limited the signal-to-noise of the NH transitions.

The frequencies of the NH lines were obtained from the spectrum using DECOMP, a data reduction program developed at the National Solar Observatory. This program contains both a line list feature which provides the frequencies of all lines above a given intensity, and a least-squares fitting procedure which uses Voigt lineshape functions to determine the true positions for all the components of blended lines.

The width (FWHM) of the lines varied from 0.17 cm^{-1} for the low-J 0–0 band to 0.23 cm^{-1} for the high-J 0–0 band to 0.25 cm^{-1} for the high-J 2–2 band. This is partly due to a range of temperatures found within the hollow cathode. However, the last three or four lines in each band show a rapid increase in linewidth from ~0.200 to ~0.250 cm^{-1}. These lines are affected by predissociation by the repulsive $^5\Sigma^-$ state. Application of the uncertainty principle to the $N' = 31$, $v' = 0$ level of $A^3\Pi$ with the known lifetime of 96 nsec (*52*) results in a broadening of only 1.6 MHz (0.00005 cm^{-1}). This is much less than the observed excess broadening of this level (0.227–0.200 = 0.027 cm^{-1}). A plausible explanation is that the levels affected by predissociation are very pressure sensitive, but further work is required to confirm this speculation.

The observed line positions of the $A^3\Pi$–$X^3\Sigma^-$ 0–0, 1–1, 2–2, 1–0, 2–1, 0–1, and 1–2 bands are given in Tables I–VII, respectively. The unblended lines have a precision of linewidth/signal-to-noise while blended lines are somewhat less precise. Virtually all of the Q-branch lines are blended to some extent while the P and R branches experience overlap from satellite lines at low J and a crossing of the three spin components at higher J.

The $A^3\Pi$–$X^3\Sigma^-$ system of NH is a good example of a Hund's case (b) to Hund's case (b) electronic transition at high J. (See Herzberg (*73*) for an explanation of coupling cases, and branch structure and notation for a $^3\Pi$–$^3\Sigma^-$ transition.) Each vibrational band has 9 strong transitions, P_1, P_2, P_3; Q_1, Q_2, Q_3; and R_1, R_2, R_3, with the tripling of the P, Q, and R branches due to electron spin. These are the only branches allowed in a pure case (b) to case (b) band, however, at lower J a transition to case (a) coupling in the $A^3\Pi$ state occurs and weak satellite branches become allowed. There are a total of 18 possible satellite branches of which 14, 11, and 9 were seen for the 0–0, 1–1, and 2–2 bands, respectively. In the 0–0 band Dixon (*3*) observed the same number of branches, but we were able to follow them to higher J, while only a few 1–1 satellite lines were seen by Murai and Shimauchi (*4*). The 2–2 band of NH has not previously been observed at high resolution. No satellite branches were measured in the $\Delta v = \pm 1$ bands, although several weak lines were observed. The signal-to-noise of these satellite lines was at best 5 to 1, and the other data from diagonal bands was sufficiently good to predict their positions much more accurately than they could be measured.

Each vibrational band was initially fitted separately using a nonlinear least-squares procedure. The Hamiltonian matrix for each state was set up using case (a) basis

TABLE I

Observed Transitions in the $A^3\Pi$–$X^3\Sigma^-$ 0–0 Band of NH

J	$P_1(J)$		$P_2(J)$		$P_3(J)$		$Q_1(J)$		$Q_2(J)$		$Q_3(J)$		$R_1(J)$		$R_2(J)$		$R_3(J)$	
	ν	Δν	ν	Δν	ν	Δν	ν	Δν	ν	Δν	ν	Δν	ν	Δν	ν	Δν	ν	Δν
0																	29848.0546	0.0007
1					29729.3801	-0.0009			29773.2630	0.0034	29783.9476	0.0038	29770.6222	0.0008	29833.8017	0.0019	29874.0514	-0.0001
2			29708.6101	0.0013	29684.0059	-0.0033	29738.1050	0.0004	29767.4302	0.0011	29777.3882	0.0019	29809.8176	0.0000	29863.3655	-0.0003	29902.8704	0.0004
3	29672.9041	0.0004	29670.6064	0.0010	29645.5843	-0.0005	29744.5180	-0.0008	29764.1562	-0.0009	29773.4404	-0.0024	29846.2710	-0.0004	29894.1272	-0.0001	29932.7330	-0.0004
4	29646.8110	-0.0008	29635.1783	-0.0007	29609.7878	0.0001	29748.2360	0.0012	29762.1948	-0.0030	29770.6781	0.0004	29881.2117	0.0001	29925.3643	-0.0001	28963.0204	-0.0001
5	29618.2396	0.0001	29601.2326	-0.0003	29575.3425	0.0001	29750.4892	-0.0010	29760.8356	-0.0013	29768.5078	-0.0001	29915.1870	0.0001	29956.7054	0.0003	29993.4119	-0.0001
6	29588.4554	0.0001	29568.1271	-0.0001	29541.7489	0.0008	29751.8737	0.0007	29759.7290	-0.0035	29766.6454	-0.0011	29948.4473	-0.0001	29987.9411	0.0002	30023.7106	0.0001
7	29558.0777	-0.0003	29535.5695	-0.0001	29508.7743	-0.0001	29752.6752	-0.0014	29758.7105	-0.0023	29764.9307	-0.0002	29981.1040	0.0001	30018.9357	-0.0006	30053.7763	0.0003
8	29527.4337	0.0002	29503.4295	-0.0006	29476.3043	-0.0006	29753.0562	0.0005	29757.6794	-0.0026	29763.2589	0.0008	30013.1980	0.0008	30049.5905	0.0002	30083.4982	0.0006
9	29496.7101	0.0003	29471.6509	0.0002	29444.2774	0.0001	29753.0938	0.0000	29756.5828	0.0037	29761.5556	0.0005	30044.7291	0.0000	30079.8178	-0.0001	30112.7802	-0.0002
10	29466.0245	0.0003	29440.2065	0.0001	29412.6565	0.0001	29752.8370	0.0018	29755.3639	0.0046	29759.7664	0.0010	30075.6787	0.0000	30109.5423	-0.0001	30141.5376	-0.0002
11	29435.4546	0.0002	29409.0876	0.0003	29381.4208	0.0000	29752.3007	0.0001	29753.9920	0.0063	29757.8411	0.0003	30106.0101	-0.0002	30138.6901	-0.0001	30169.6881	0.0002
12	29405.0543	0.0003	29378.2894	-0.0003	29350.5557	-0.0002	29751.4918	-0.0033	29752.4296	0.0053	29755.7364	-0.0013	30135.6785	-0.0001	30167.1892	0.0002	30197.1511	0.0000
13	29374.8604	-0.0002	29347.8118	0.0000	29320.0497	-0.0001	29750.4123	-0.0012	29750.6377	-0.0040	29753.4112	-0.0027	30164.6305	0.0000	30194.9661	-0.0001	30223.8478	-0.0002
14	29344.9000	-0.0002	29317.6511	0.0000	29289.8911	0.0002	29749.0418	-0.0005	29748.6005	-0.0031	29750.8233	-0.0038	30192.8074	0.0000			30249.6997	0.0010
15	29315.1896	-0.0001	29287.8033	0.0001	29260.0663	0.0002	29747.3596	-0.0018	29746.2737	0.0001	29747.9344	0.0004	30220.1452	-0.0003	30248.0587	0.0000	30274.6217	0.0000
16	29285.1381	-0.0003	29258.2601	0.0000	29230.5592	-0.0001	29745.3449	-0.0002	29743.6132	0.0002	29744.6871	-0.0014	30246.5771	0.0002	30273.2201	-0.0001	30298.5326	-0.0007
17	29256.5479	-0.0007	29229.0102	0.0000	29201.3512	-0.0001	29742.9650	0.0026	29740.5840	0.0045	29741.0436	0.0016	30272.0294	0.0003	30297.3493	-0.0020	30321.3468	-0.0001
18	29227.6161	-0.0001	29200.0376	0.0002	29172.4183	0.0002	29740.1743	-0.0027	29737.1273	0.0002	29736.9431	0.0015	30296.4257	0.0002	30320.3688	0.0012	30342.9724	0.0002
19	29198.9311	0.0001	29171.3195	-0.0010	29143.7311	0.0002	29736.9486	0.0008	29733.2083	0.0028	29732.3320	0.0017	30319.6860	0.0008	30342.1791	-0.0014	30363.3165	0.0017
20	29170.4761	-0.0001	29142.8327	0.0000	29115.2551	0.0001	29733.2253	-0.0026	29728.7609	0.0013	29727.1461	0.0005	30341.7221	-0.0001	30362.6939	-0.0030	30382.2812	0.0063
21	29142.2286	0.0002	29114.5395	-0.0015	29086.9489	-0.0004	29728.9688	0.0036	29723.7264	-0.0020	29721.3197	0.0005	30362.4435	-0.0028	30381.8196	0.0012	30399.7432	-0.0039
22	29114.1548	-0.0028	29086.4057	0.0000	29058.7672	0.0016	29724.1008	-0.0002	29718.0444	-0.0004	29714.7720	-0.0037	30381.7551	-0.0049	30399.4447	0.0045	30415.6150	-0.0038
23	29086.2284	0.0022	29058.3758	-0.0039	29030.6495	0.0021	29718.5693	-0.0008	29711.6343	-0.0003	29707.4306	-0.0014	30399.5630	0.0024	30415.4488	-0.0019	30429.7675	-0.0016
24	29058.3921	0.0032	29030.4113	0.0037	29002.5287	-0.0009			29704.4151	-0.0004	29699.1955	-0.0001	30415.7319	-0.0055	30429.7299	0.0003	30442.0703	0.0024
25	29030.5917	-0.0001	29002.4186	-0.0062	28974.3377	0.0011	29705.2099	0.0004	29696.2966	0.0007	29689.9642	0.0003	30430.1747	0.0034	30442.1487	0.0014	30452.3742	0.0003
26	29002.7718	0.0002	28974.3510	-0.0057	28945.9788	-0.0029	29697.2081	0.0000	29687.1769	0.0031	29679.6244	0.0020	30442.7336	0.0001	30452.5628	-0.0001	30460.5314	-0.0014
27	28974.8546	0.0000	28946.1141	-0.0028	28917.3669	0.0013	29688.1983	0.0036	29676.9293	-0.0058	29668.0458	0.0030	30453.2813	-0.0025	30460.8223	-0.0004	30466.3796	0.0044
28	28946.7551	-0.0003	28917.6055	-0.0011	28888.3761	0.0020	29678.0563	0.0003	29665.4504	-0.0017			30461.6673	-0.0016	30466.7685	0.0110	30469.7072	-0.0074
29	28918.3758	0.0000	28888.7134	0.0013	28858.8781	0.0010	29666.6632	-0.0015	29652.5780	-0.0031			30467.7264	0.0058	30470.1760	-0.0050	30470.3358	-0.0079
30	28889.6038	0.0010	28859.3060	0.0025	28828.7263	0.0009	29653.8796	0.0018					30471.2656	0.0130	30470.8753	-0.0110	30468.0095	-0.0225
31	28860.3093	0.0024	28829.2369	0.0049	28797.7525	0.0038	29639.5084	-0.0255					30472.0612	0.0026			30462.4762	-0.0453
32	28830.3352	-0.0046	28798.3265	-0.0010	28765.7403	-0.0121												
33	28799.5233	-0.0086	28766.3723	-0.0232														
34	28767.6710	-0.0180																

J	$^{Q}P_{12}(J)$		$^{Q}P_{23}(J)$		$^{Q}P_{21}(J)$		$^{Q}P_{32}(J)$		$^{P}Q_{12}(J)$		$^{P}Q_{23}(J)$		$^{R}Q_{21}(J)$	
	ν	Δν	ν	Δν	ν	Δν	ν	Δν	ν	Δν	ν	Δν	ν	Δν
1							29796.1998	-0.0059			29709.7178	-0.0005	29807.2803	-0.0027
2			29610.9921	-0.0080	29774.1062	-0.0040	29782.8337	-0.0007	29671.9479	0.0007	29671.5436	0.0032	29834.6491	-0.0014
3	29574.0602	0.0007	29540.0687	-0.0031	29768.3769	-0.0087	29776.4536	0.0023	29645.7724	-0.0002	29636.0074	-0.0011	29864.3214	-0.0009
4	29515.3755	-0.0001	29472.0066	-0.0032			29772.6132	-0.0001	29617.1285	0.0004	29601.9759	-0.0042	29895.1660	-0.0006
5	29454.3014	0.0003	29405.6376	0.0014	29763.3086	-0.0005	29769.9295	-0.0010			29568.8042	0.0014	29926.4759	0.0002
6	29392.1459	0.0041	29340.3123	0.0006	29762.0158	0.0015	29767.8288	-0.0035	29556.8384	0.0000	29536.1826	0.0027	29957.8864	0.0039
7	29329.5584	-0.0017	29275.7651	-0.0054			29766.0313	-0.0049	29526.1337	-0.0008	29503.9824	0.0035	29989.1795	-0.0010
8	29266.9213	-0.0049	29211.9128	-0.0046					29495.3512	-0.0024	29472.1448	0.0038	30020.2338	-0.0016
9	29204.4730	0.0020	29148.7306	-0.0016	29759.0368	-0.0015			29464.6130	0.0005	29440.6444	0.0039	30050.9451	-0.0015
10									29433.9889	0.0000	29409.4722	0.0052	30081.2322	0.0026
11	29080.6914	-0.0015							29403.5353	-0.0010	29378.6176	0.0008	30111.0068	-0.0010
12									29373.2965	0.0043			30140.2079	0.0001
13									29343.2820	-0.0005			30168.7568	-0.0006
14									29313.5285	0.0042			30196.5865	0.0026
15									29284.0311	0.0044				
16									29254.7962	0.0041				
17														
18									29197.0872	-0.0027				
19									29168.5963	0.0012				

J	$^{R}Q_{32}(J)$		$^{Q}R_{12}(J)$		$^{Q}R_{23}(J)$		$^{S}R_{21}(J)$		$^{S}R_{32}(J)$		$^{R}P_{31}(J)$		$^{O}Q_{13}(J)$	
	ν	Δν	ν	Δν	ν	Δν	ν	Δν	ν	Δν	ν	Δν	ν	Δν
0					29775.0400	-0.0048								
1	29846.2710	0.0023	29737.2532	-0.0007	29768.5429	0.0044	29866.1003	-0.0030	29939.6520	0.0063	29826.9478	0.0021		
2	29872.9422	0.0001	29743.5660	0.0036			29928.2015	-0.0006	30000.8015	0.0015	29847.1207	0.0014	29574.9889	-0.0056
3	29901.9348	-0.0002	29747.1918	-0.0037	29763.0318	0.0046	29991.3376	-0.0034	30062.8298	0.0049				
4	29931.9034	-0.0005	29749.3782	-0.0007			30054.7710	0.0004	30125.0785	0.0090				
5	29962.2734	0.0001	29750.6958	0.0002	29760.4008	-0.0073	30118.0814	0.0004						
6	29992.7369	0.0006			29759.3232	0.0001	30181.0271	0.0014						
7	30023.0980	-0.0022												
8	30053.2289	0.0017												
9	30083.0091	0.0018												
10	30112.3423	-0.0040												
11			29750.8374	0.0023										
12														
13			29748.8411	-0.0040										

TABLE II

Observed Transitions in the $A^3\Pi$–$X^3\Sigma^-$ 1–1 Band of NH

J	$P_1(J)$		$P_2(J)$		$P_3(J)$		$Q_1(J)$		$Q_2(J)$		$Q_3(J)$		$R_1(J)$		$R_2(J)$		$R_3(J)$	
	ν	Δν	ν	Δν	ν	Δν	ν	Δν	ν	Δν	ν	Δν	ν	Δν	ν	Δν	ν	Δν
1					29641.0578	0.0152			29682.0912	-0.0048	29692.7071	0.0021	29678.0922	0.0038	29739.7818	-0.0035	29778.3857	0.0008
2			29619.9738	-0.0055	29596.7177	0.0034	29646.8602	-0.0021	29676.0697	-0.0008	29685.5622	-0.0009	29715.5773	-0.0008	29767.4919	-0.0009	29805.0889	-0.0006
3	29584.2453	0.0002	29583.0556	-0.0004	29558.9733	0.0021	29652.8691	0.0007	29672.2422	-0.0023	29680.8111	-0.0037	29750.1630	0.0029	29796.1612	0.0051	29832.6371	0.0009
4	29559.0327	0.0010	29548.3535	0.0001	29523.6388	0.0002	29656.0117	-0.0044	29669.4932	0.0001	29677.0423	0.0015	29783.0247	-0.0029	29825.0881	0.0047	29860.4010	0.0000
5	29531.1701	0.0004	29514.8868	-0.0006	29489.4492	-0.0008	29657.5053	-0.0009	29667.1346	0.0039	29673.6497	-0.0069	29814.7195	-0.0005	29853.9061	0.0005	29888.0589	0.0000
6	29501.8912	0.0000	29482.0447	-0.0007	29455.9017	0.0008	29657.9163	0.0001	29664.8174	-0.0001	29670.3678	-0.0018	29845.4827	-0.0005	29882.4098	0.0000	29915.4023	-0.0034
7	29471.8048	0.0004	29449.5375	0.0006	29422.7546	0.0003	29657.5359	0.0014	29662.3776	0.0003	29667.0069	-0.0034	29875.4261	0.0020	29910.4541	-0.0002	29942.2933	-0.0002
8	29441.2303	0.0000	29417.2267	0.0002	29389.8860	-0.0002	29656.5106	-0.0006	29659.7067	-0.0005	29663.4648	-0.0027	29904.5777	-0.0002	29937.9305	0.0001	29968.6024	0.0000
9	29410.3515	-0.0001	29385.0494	0.0002	29357.2249	-0.0004	29654.9239	0.0000	29656.7375	-0.0008	29659.6598	0.0009	29932.9379	-0.0022	29964.7452	0.0008	29994.2273	0.0002
10	29379.2797	0.0001	29352.9717	0.0002	29324.7266	-0.0001	29652.8120	0.0021	29653.4166	0.0000	29655.5190	0.0014	29960.4814	-0.0002	29990.8098	0.0005	30019.0691	-0.0005
11	29348.0836	-0.0008	29320.9741	0.0003	29292.3579	-0.0003	29650.1823	0.0008	29649.6934	-0.0015	29650.9841	0.0004	29987.1579	0.0005	30016.0399	-0.0002	30043.0356	0.0009
12	29316.8091	-0.0019	29289.0413	-0.0005	29260.0913	-0.0016	29647.0323	-0.0019	29645.5241	-0.0034	29646.0016	0.0016	30012.9078	-0.0031	30040.3515	0.0003	30066.0300	0.0023
13	29285.4881	0.0013	29257.1617	0.0003	29227.9044	-0.0010	29643.3518	0.0005	29640.8676	0.0000	29640.5106	0.0012	30037.6765	0.0002	30063.6548	-0.0004	30087.9519	0.0000
14	29254.1263	0.0002	29225.3167	0.0001	29195.7688	0.0003	29639.1086	0.0022	29635.6656	-0.0003	29634.4511	-0.0014	30061.3803	0.0002	30085.8603	-0.0006	30108.7094	0.0014
15	29222.7327	0.0001	29193.4860	-0.0015	29163.6516	-0.0001	29634.2685	0.0037	29629.8692	0.0001	29627.7646	-0.0018	30083.9431	0.0014	30106.8713	-0.0019	30128.1920	-0.0001
16	29191.2988	-0.0014	29161.6493	0.0003	29131.5195	0.0000	29628.7857	0.0019	29623.4212	0.0022	29620.3831	-0.0004	30105.2722	-0.0014	30126.5918	0.0002	30146.2951	-0.0001
17	29159.8145	0.0002	29129.7717	0.0019	29099.3302	-0.0002	29622.6141	0.0009	29616.2521	0.0005	29612.2305	0.0005	30125.2802	-0.0010	30144.9074	-0.0023	30162.9020	0.0003
18	29128.2517	0.0003	29097.8114	-0.0002	29067.0349	-0.0006	29615.6952	0.0002	29608.2944	-0.0016	29603.2239	-0.0009	30143.8598	-0.0029	30161.7144	0.0003	30177.8884	-0.0002
19	29096.5788	-0.0003	29065.7281	-0.0002	29034.5783	0.0007	29607.9631	0.0000	29599.4741	0.0004	29593.2824	0.0035	30160.9033	-0.0050	30176.8832	-0.0002	30191.1272	0.0032
20	29064.7559	0.0003	29033.4644	-0.0002	29001.8903	0.0003	29599.3414	-0.0014	29589.6976	0.0003	29582.2969	0.0035	30176.2920	-0.0073	30190.2876	0.0006	30202.4650	-0.0009
21	29032.7310	0.0015	29000.9555	-0.0002	28968.8947	-0.0006	29589.7502	0.0006	29578.8696	-0.0002	29570.1607	0.0019	30189.9090	0.0015	30201.7882	0.0041	30211.7605	-0.0001
22	29000.4382	-0.0002	28968.1284	0.0030	28935.5053	0.0009	29579.0856	-0.0032	29566.8811	-0.0017			30201.5919	-0.0019	30211.2253	0.0034		
23	28967.8098	0.0010	28934.8839	-0.0017	28901.6105	-0.0040	29567.2387	-0.0153	29553.6148	-0.0007			30211.2023	-0.0047				
24	28934.7543	0.0002	28901.1321	-0.0026			29554.1171	-0.0088	29538.9243	-0.0088								
25	28901.1740	-0.0003					29539.5820	0.0111	29522.6874	0.0026								

J	$^{O}P_{12}(J)$		$^{O}P_{23}(J)$		$^{P}P_{21}(J)$		$^{Q}P_{32}(J)$		$^{P}Q_{12}(J)$		$^{P}Q_{23}(J)$	
	ν	Δν	ν	Δν	ν	Δν	ν	Δν	ν	Δν	ν	Δν
1											29621.0879	-0.0079
2			29526.3038	-0.0077	29682.9363	-0.0057	29691.5932	0.0047	29583.2965	0.0003	29583.9998	-0.0010
3			29457.7807	0.0075	29677.0205	0.0011	29684.6184	0.0001	29558.0047	0.0018	29549.1962	0.0007
4	29432.7798	-0.0003	29391.7287	-0.0097			29679.9701	-0.0026	29530.0731	0.0013	29515.6479	-0.0021
5	29373.7222	0.0036	29327.1477	-0.0013			29676.2729	-0.0053	29500.7314	0.0013	29482.7389	-0.0004
6	29313.3767	0.0064	29263.3897	-0.0036					29470.5857	0.0016	29450.1667	-0.0015
7											29417.8005	0.0013
8									29409.0132	-0.0073	29385.5690	0.0029
9							29662.9470	-0.0036	29377.8855	-0.0105	29353.4385	0.0037
10									29346.6522	0.0022	29321.3828	-0.0028
11											29289.3954	-0.0083
12									29283.9514	-0.0041		

J	$^{R}Q_{21}(J)$		$^{R}Q_{32}(J)$		$^{Q}R_{12}(J)$		$^{Q}R_{23}(J)$		$^{S}R_{21}(J)$	
	ν	Δν	ν	Δν	ν	Δν	ν	Δν	ν	Δν
1					29646.0159	-0.0004	29677.1857	-0.0012	29770.8568	-0.0059
2					29651.9201	0.0006	29673.1932	0.0039	29829.8184	-0.0013
3			29804.1508	0.0061			29670.3315	-0.0037	29889.5837	0.0023
4	29797.1832	-0.0017	29831.7953	0.0012			29667.8863	-0.0070	29949.4249	-0.0033
5	29826.1811	-0.0002	29859.6375	-0.0008			29665.5071	-0.0043		
6	29855.0638	-0.0031	29887.3666	0.0016			29663.0215	0.0129	30067.8984	-0.0086
7	29883.6399	0.0098	29914.7708	-0.0036						
8	29911.7311	-0.0001	29941.7249	0.0040	29653.5793	-0.0135				
9	29939.2631	0.0015			29651.4309	0.0046				
10	29966.1334	0.0054								

TABLE III

Observed Transitions in the $A^3\Pi$–$X^3\Sigma^-$ 2–2 Band of NH

J	$P_1(J)$		$P_2(J)$		$P_3(J)$		$Q_1(J)$		$Q_2(J)$		$Q_3(J)$		$R_1(J)$		$R_2(J)$		$R_3(J)$	
	ν	Δν	ν	Δν	ν	Δν	ν	Δν	ν	Δν	ν	Δν	ν	Δν	ν	Δν	ν	Δν
0																	29619.6798	-0.0053
1									29550.1631	0.0010	29560.5930	-0.0037	29544.7832	0.0005	29604.8806	-0.0036	29641.6824	0.0060
2			29490.5675	-0.0006	29468.5802	0.0046			29543.8332	-0.0025	29552.6713	0.0010	29580.4303	0.0003	29630.5488	0.0063		
3	29454.8128	0.0038	29454.6142	0.0012	29431.3066	-0.0005	29520.3061	-0.0004	29539.2662	0.0002	29546.8460	0.0005	29612.9448	0.0014			29690.8806	0.0009
4	29430.3337	-0.0019	29420.4407	-0.0002	29396.1643	0.0012	29522.6877	-0.0010	29535.4568	-0.0001			29643.4705	-0.0033			29715.7146	0.0085
5	29402.9846	-0.0002	29387.1861	-0.0005	29361.8868	0.0003	29523.1522	0.0027	29531.7553	0.0002	29536.7086	0.0000			29709.0116	0.0014		
6	29373.9456	0.0001	29354.2662	-0.0018	29327.9733	0.0066	29522.2488	-0.0041	29527.8225	0.0001	29531.5084	0.0007	29700.4020	-0.0027	29734.2935	0.0006		
7	29343.8130	0.0004	29321.3956	0.0005	29294.1562	-0.0006	29520.2806	0.0008	29523.4802	0.0048	29525.9387	0.0006	29727.1459	0.0024			29787.0148	0.0005
8	29312.8972	-0.0020	29288.4274	0.0021	29260.3078	-0.0137	29517.3720	-0.0003	29518.6009	-0.0003	29519.8741	-0.0016			29782.4459	-0.0120	29809.1650	0.0034
9	29281.3791	-0.0011	29255.2844	0.0017	29226.3753	-0.0009	29513.5993	0.0004	29513.1187	0.0005	29513.2263	0.0024			29805.1162	0.0061	29830.2765	-0.0044
10	29249.3579	0.0009	29221.9197	-0.0014	29192.2571	-0.0036			29506.9575	-0.0005	29505.9005	0.0020	29800.7142	-0.0016	29826.6658	-0.0025	29850.2535	-0.0008
11	29216.8801	-0.0080	29188.3050	-0.0008	29157.9268	0.0013			29500.0526	-0.0038	29497.8192	-0.0013	29822.8950	0.0049			29868.9734	0.0092
12	29184.0033	-0.0010	29154.4089	0.0035	29123.3254	0.0014	29497.2154	0.0026	29492.3504	0.0018	29488.9146	0.0036	29843.7822	0.0064				
13	29150.7119	-0.0046	29120.1905	0.0042	29088.4138	0.0054	29490.0013	0.0034	29483.7605	-0.0057	29479.0873	-0.0010						
14	29117.0212	0.0014	29085.6082	-0.0020	29053.1253	-0.0012			29474.2410	0.0056	29468.2592	-0.0065						
15	29082.8995	0.0034	29050.6299	-0.0022	29017.4190	-0.0006			29463.6671	-0.0085								
16	29048.3247	0.0100																

J	$^0P_{12}(J)$		$^QP_{21}(J)$		$^QP_{32}(J)$		$^PQ_{12}(J)$		$^PQ_{23}(J)$		$^RQ_{21}(J)$		$^RQ_{32}(J)$		$^QR_{12}(J)$		$^QR_{23}(J)$	
	ν	Δν	ν	Δν	ν	Δν	ν	Δν	ν	Δν	ν	Δν	ν	Δν	ν	Δν	ν	Δν
0																	29551.9465	-0.0049
1									29491.6886	0.0013	29581.4771	-0.0035	29617.9029	0.0070	29514.0130	0.0064	29544.9472	-0.0076
2			29550.9974	-0.0036	29559.4825	0.0050	29453.8703	0.0001	29455.5612	-0.0027	29605.7151	-0.0079			29519.3676	-0.0001		
3			29544.7698	-0.0046	29551.7194	0.0000	29429.3254	0.0054	29421.2923	-0.0001	29631.4873	0.0060			29521.6729	-0.0001	29536.3060	-0.0024
4	29309.2579	-0.0082			29545.9916	-0.0024	29401.9101	0.0071	29387.9630	0.0010							29532.5253	-0.0052
5					29540.9426	-0.0029	29372.8012	-0.0023	29354.9868	0.0087					29521.1060	-0.0048		
6			29532.8978	0.0007			29342.6169	0.0026	29322.0446	-0.0015					29519.0758	-0.0058		
7			29529.0216	0.0030			29311.6595	0.0119			29735.4973	0.0061						
8			29524.7220	-0.0050														

TABLE IV

Observed Transitions in the $A^3\Pi$–$X^3\Sigma^-$ 1–0 Band of NH

J	$P_1(J)$		$P_2(J)$		$P_3(J)$		$Q_1(J)$		$Q_2(J)$		$Q_3(J)$		$R_1(J)$		$R_2(J)$		$R_3(J)$	
	ν	Δν	ν	Δν	ν	Δν	ν	Δν	ν	Δν	ν	Δν	ν	Δν	ν	Δν	ν	Δν
1													32803.6627	0.0017	32864.0593	-0.0032	32900.0684	-0.0002
2					32714.5250	0.0085	32771.1500	0.0058	32797.7545	-0.0066	32803.3678	0.0025	32839.8617	0.0017	32889.1801	-0.0033	32922.9007	0.0090
3	32705.9538	0.0105	32700.8671	-0.0010	32671.6026	0.0008	32774.5652	-0.0014	32790.0581	0.0015	32793.4398	-0.0056	32871.8624	0.0041	32913.9686	0.0005	32945.2709	0.0041
4	32676.8527	-0.0015	32660.9925	-0.0042	32629.8165	0.0070	32773.8403	0.0016	32782.1344	-0.0019	32783.2076	-0.0041	32900.8482	-0.0019	32937.7234	-0.0033	32966.5712	-0.0007
5	32643.8255	-0.0009	32621.0807	0.0070	32587.8784	0.0026	32770.1647	0.0018	32773.3145	-0.0026	32772.0796	-0.0029			32960.0961	0.0042	32986.4832	-0.0015
6	32608.0905	-0.0034	32580.4867	-0.0028	32545.2989	-0.0006	32764.1185	-0.0003	32763.2554	-0.0062	32759.7615	-0.0067	32951.6876	0.0017	32980.8506	-0.0032	33004.8044	0.0001
7	32570.2655	-0.0022	32538.9515	-0.0050	32501.8433	-0.0038	32755.9979	0.0001	32751.7940	-0.0028	32746.0941	-0.0090	32973.8880	0.0006	32999.8710	-0.0029	33021.3860	-0.0002
8	32530.6723	0.0003	32452.5880	-0.0002	32457.3946	-0.0041	32745.9524	-0.0005	32738.8193	-0.0044	32730.9712	-0.0088	32994.0200	0.0003	33017.0466	-0.0003	33036.1097	-0.0052
9	32489.4865	-0.0068	32407.6553	-0.0078	32411.8848	-0.0028	32734.0680	0.0024	32724.2742	-0.0031	32714.3137	-0.0075	33012.0816	-0.0001	33032.2852	0.0017	33048.8825	-0.0069
10	32446.8463	-0.0004	32361.5499	-0.0029	32365.2677	-0.0060	32720.3794	0.0024	32708.1057	-0.0025	32696.0608	-0.0038	33028.0464	-0.0023	33045.5025	0.0016	33059.6132	-0.0033
11	32402.8065	-0.0005	32314.2447	-0.0035	32317.5287	-0.0011	32704.9104	0.0063	32690.2708	-0.0031	32676.1482	-0.0071	33041.8754	-0.0046	33056.6146	-0.0044	33068.2044	-0.0020
12	32357.4258	0.0018	32265.7353	-0.0054	32268.6327	-0.0020	32687.6496	0.0024	32670.7328	-0.0011	32654.5320	-0.0097	33053.5240	0.0001	33065.5608	0.0031	33074.5653	-0.0041
13	32310.7256	-0.0047	32216.0204	0.0006	32218.5657	-0.0026	32668.5934	-0.0013	32649.4492	0.0024	32631.1672	-0.0050	33062.9178	-0.0019	33072.2368	0.0023	33078.6071	-0.0077
14	32262.7490	0.0035	32165.0701	-0.0013	32167.3105	0.0013	32647.7278	0.0020	32626.3750	0.0059	32605.9908	-0.0024	33070.0101	0.0106	33076.5599	-0.0042	33080.2331	-0.0156
15	32213.4800	0.0011	32112.8781	0.0020	32114.8308	-0.0020	32625.0122	0.0010	32601.4546	0.0016	32578.9459	-0.0017	33074.6882	0.0002	33078.4517	-0.0054	33079.3744	0.0012
16	32162.9308	0.0004	32059.4044	-0.0041	32061.1021	-0.0072	32600.4135	-0.0005			32549.9753	0.0020	33076.9064	0.0026	33077.8213	0.0025	33075.8781	-0.0068
17	32111.0862	-0.0049							32545.8845	-0.0059	32519.0001	-0.0022			33074.5653	0.0168	33069.6615	-0.0126
18	32057.9398	-0.0033					32545.3837	-0.0030	32515.1094	-0.0110	32485.9407	-0.0184	33073.5478	-0.0066	33068.5357	-0.0028		
19							32514.8339	-0.0100					33067.7798	-0.0093				

TABLE V

Observed Transitions in the $A^3\Pi$–$X^3\Sigma^-$ 2–1 Band of NH

J	$P_1(J)$		$P_2(J)$		$P_3(J)$		$Q_1(J)$		$Q_2(J)$		$Q_3(J)$		$R_1(J)$		$R_2(J)$		$R_3(J)$	
	ν	Δν	ν	Δν	ν	Δν	ν	Δν	ν	Δν	ν	Δν	ν	Δν	ν	Δν	ν	Δν
1													32514.0802	-0.0054				
2							32482.8552	-0.0043	32509.2468	-0.0120	32514.2079	-0.0051	32548.4428	-0.0013	32595.9620	-0.0037	32627.5356	-0.0004
3			32416.1416	-0.0202	32387.6812	-0.0019	32485.7418	0.0020	32500.8109	-0.0040	32503.2273	0.0057	32578.3738	-0.0029	32618.3871	-0.0031	32647.2568	0.0010
4			32376.8041	-0.0222	32346.0882	0.0030	32484.2568	0.0062	32491.8485	0.0062	32491.6585	0.0156	32605.0409	0.0051	32639.4972	-0.0080	32665.6334	0.0052
5	32359.3910	0.0047	32337.1130	-0.0084	32304.0611	-0.0085	32479.5507	-0.0003	32481.6908	0.0009	32478.9005	0.0089	32628.9536	0.0041	32658.9392	-0.0058	32682.3138	-0.0078
6	32323.8876	-0.0117	32296.4596	-0.0076	32261.1197	-0.0084	32472.2114	0.0047	32470.0068	-0.0148	32464.6738	0.0046	32650.3598	0.0012	32676.4861	-0.0060	32697.1162	-0.0069
7	32286.0228	-0.0111	32254.5596	-0.0167			32462.5003	-0.0008	32456.6583	0.0017	32448.8089	0.0106	32669.3569	-0.0079	32691.9988	0.0016		
8	32246.0962	-0.0095	32211.3105	0.0016			32450.5737	-0.0051	32441.4683	-0.0165	32431.1536	-0.0042	32685.9938	-0.0029				
9	32204.2928	0.0005	32166.5909	-0.0012	32124.8112	0.0050	32436.5053	-0.0058	32424.4158	-0.0117	32411.6553	0.0014	32700.2341	-0.0067				
10	32160.6848	-0.0135	32120.3914	0.0089			32420.3224	-0.0043	32405.4018	-0.0177								

TABLE VI

Observed Transitions in the $A^3\Pi$–$X^3\Sigma^-$ 0–1 Band of NH

J	$P_1(J)$		$P_2(J)$		$P_3(J)$		$Q_1(J)$		$Q_2(J)$		$Q_3(J)$		$R_1(J)$		$R_2(J)$		$R_3(J)$	
	ν	Δν	ν	Δν	ν	Δν	ν	Δν	ν	Δν	ν	Δν	ν	Δν	ν	Δν	ν	Δν
2							26613.8240	0.0013							26741.6746	-0.0006	26820.1042	0.0014
3	26551.1870	-0.0185	26552.7828	-0.0106	26532.9605	0.0063	26622.8080	-0.0127	26646.3485	0.0035			26724.5679	-0.0053	26776.3209	0.0056	26856.8391	-0.0105
4	26528.9849	-0.0044	26522.5332	-0.0026	26503.6335	0.0167	26630.4127	0.0005	26649.5563	0.0018	26664.5255	0.0187	26763.4008	0.0117	26812.7226	0.0015	26894.9865	0.0003
5	26505.5779	-0.0049	26495.0431	-0.0034	26476.9252	0.0086	26637.8318	-0.0018	26654.6306	-0.0199	26670.0972	0.0151	26802.5298	-0.0005			26934.3089	-0.0031
6	26482.2497	-0.0030	26469.6877	0.0046	26452.3481	-0.0015	26645.6697	-0.0006			26677.2623	0.0143	26842.2451	0.0004	26889.5122	0.0154	26974.6629	-0.0204
7	26459.6144	-0.0003	26446.1480	-0.0021	26429.6807	-0.0009	26654.2148	0.0015	26669.2910	-0.0022	26685.8454	0.0072	26882.6439	0.0033	26929.5149	-0.0019	27015.9703	-0.0149
8	26437.9851	-0.0067	26424.3124	-0.0012	26408.7886	-0.0038	26663.6136	-0.0003	26678.5564	-0.0091	26695.7441	-0.0015	26923.7655	0.0100	26970.4698	-0.0039	27058.0991	-0.0190
9	26417.5638	-0.0044	26404.1126	0.0010	26389.6035	-0.0116	26673.9514	-0.0008	26689.0406	0.0006	26706.8859	-0.0069	26965.5845	-0.0029	27012.2861	0.0072	27100.9931	0.0023
10	26398.4502	-0.0069	26385.5203	0.0055	26372.0964	-0.0131	26685.2608	-0.0073	26700.6597	-0.0080	26719.2158	-0.0026	27008.1216	0.0100	27054.8461	-0.0047		
11	26380.7251	-0.0067	26368.4978	-0.0105	26356.2401	-0.0091	26697.5738	-0.0041	26713.3941	-0.0126	26732.6694	0.0002	27051.2861	-0.0016	27098.1140	0.0028	27188.5961	-0.0133
12	26364.4364	-0.0046	26353.0878	0.0045	26342.0102	-0.0039	26710.8816	-0.0005	26727.2068	-0.0111	26747.1935	-0.0024	27095.0652	-0.0004	27141.9910	0.0084	27233.1874	0.0022
13	26349.5268	-0.0904	26339.2287	-0.0038	26329.3986	0.0116	26725.1737	0.0037	26742.0553	-0.0071	26762.7550	0.0040	27139.3953	0.0082			27278.1534	-0.0046
14	26336.2826	0.0018	26326.9473	-0.0007	26318.3592	0.0090	26740.4242	0.0013	26757.8999	-0.0005	26779.2830	-0.0034	27184.1875	-0.0005	27231.2309	-0.0140	27323.4290	-0.0116
15	26324.4386	-0.0047	26316.2245	0.0052	26308.8870	0.0020	26756.6204	0.0054	26774.7013	0.0115	26796.7557	0.0029	27229.3798	-0.0194	27276.4571	-0.0178	27368.9373	-0.0062
16	26314.1038	-0.0043	26307.0372	0.0043	26300.9773	0.0077	26773.7098	-0.0051	26792.3820	-0.0038	26815.1029	0.0041	27274.9320	-0.0147	27321.9787	-0.0144		
17	26305.2629	-0.0089	26299.3716	0.0002			26791.7017	0.0161	26810.9479	0.0072	26834.2748	0.0052	27320.7550	0.0027	27367.6901	-0.0225		
18			26293.2192	0.0061			26810.4834	-0.0019	26830.3053	0.0026	26854.2012	-0.0062	27366.7273	-0.0065	27413.5330	-0.0102		
19			26288.5589	0.0278			26830.0547	-0.0123	26850.4303	0.0142	26874.8562	0.0064	27412.7906	-0.0138				
20									26871.2260	0.0054	26896.1399	0.0099						
21									26892.6793	0.0286								

TABLE VII

Observed Transitions in the $A^3\Pi$–$X^3\Sigma^-$ 1–2 Band of NH

J	$P_1(J)$		$P_2(J)$		$P_3(J)$		$Q_1(J)$		$Q_2(J)$		$Q_3(J)$		$R_1(J)$		$R_2(J)$		$R_3(J)$	
	ν	Δν	ν	Δν	ν	Δν	ν	Δν	ν	Δν	ν	Δν	ν	Δν	ν	Δν	ν	Δν
3					26602.6042	0.0090	26687.4382	0.0031	26710.6874	-0.0082	26724.4582	0.0194	26784.7258	-0.0010	26834.5999	-0.0073		
4					26573.7095	-0.0070	26694.4494	-0.0048	26713.1053	-0.0023	26727.1328	0.0140	26821.4717	0.0061	26868.7013	0.0033	26910.4812	0.0023
5	26574.7617	-0.0065	26564.9376	-0.0150	26547.2700	0.0030	26701.1117	0.0070	26717.1879	-0.0080	26731.4705	-0.0031	26858.3195	0.0010	26903.9664	-0.0044	26945.8672	-0.0086
6	26551.9365	-0.0008	26539.8401	-0.0061	26522.7466	0.0072	26707.9622	-0.0001	26722.6141	-0.0042	26737.1942	-0.0139	26895.5289	-0.0005	26940.2142	0.0036		
7	26529.5841	0.0010	26516.3567	0.0010			26715.3110	-0.0022	26729.1833	-0.0128	26744.1355	-0.0147	26933.2065	0.0037	26977.2697	-0.0034	27019.4223	-0.0110
8	26508.0228	-0.0010	26494.3456	0.0027	26478.6029	-0.0012	26723.3111	0.0064	26736.8209	-0.0027	26752.1814	-0.0040	26971.3702	-0.0012	27015.0377	-0.0091	27057.3252	0.0049
9	26487.4399	0.0004	26473.7386	-0.0012	26458.7954	0.0002	26732.0196	0.0079	26745.4379	0.0090	26761.2103	-0.0186	27010.0339	0.0060	27053.4293	-0.0058	27095.7981	0.0011
10	26467.9464	0.0082	26454.5111	0.0011	26440.4257	0.0063	26741.4815	0.0129	26754.9606	0.0054	26771.2158	0.0055	27049.1518	0.0115	27092.3138	-0.0340		
11	26449.6129	0.0255	26436.6436	0.0128	26423.4603	0.0187	26751.6927	0.0082	26765.3625	0.0106	26782.0615	-0.0056	27088.6769	0.0165	27131.6945	-0.0026	27174.1164	-0.0017
12	26432.4404	0.0117	26420.0955	0.0107	26407.8440	0.0120	26762.6717	0.0198	26776.5744	0.0038	26793.7325	-0.0065	27128.5580	0.0294	27171.3927	-0.0016		
13	26416.5051	0.0184	26404.8710	0.0157	26393.5698	0.0075	26774.3735	0.0224	26788.5688	0.0073			27168.6854	0.0092				
14	26401.7966	0.0239	26390.9307	0.0074			26786.7692	0.0162	26801.2706	-0.0020								
15	26388.2766	-0.0109	26378.2630	-0.0033			26799.8295	0.0098										
16			26366.8590	0.0025			26813.5001	-0.0060										
17	26364.9579	-0.0026	26356.6620	0.0019														

functions and diagonalized, to produce a set of energy levels. The effective Hamiltonian for a $^3\Sigma^-$ state is given by Zare *et al.* (*74*), while Roux *et al.* (*75*) give explicit matrix elements to second order. The explicit matrix elements for a $^3\Pi$ state were taken from Brown and Merer (*76*).

Initial attempts to reproduce our data for the 0–0 band using these matrix elements proved unsuccessful. The lines were of very high precision (up to ± 0.0002 cm^{-1}) and also involved high rotational levels (up to $N = 32$ which has more than 16 000 cm^{-1} of rotational energy). As a result, many higher order distortion constants were required, for example, B, D, H, L, and M for the rotational energy, and q, q_D, q_H, and q_L for the Λ-doubling interaction. The higher order matrix elements were derived from the existing ones by multiplying the matrices, making them Hermitian where necessary. For example,

$$\mathbf{M} = M(\mathbf{B}/B)^5 \qquad \text{or} \qquad \mathbf{q}_L = q_L[(\mathbf{q}/q)(\mathbf{B}/B)^3 + (\mathbf{B}/B)^3(\mathbf{q}/q)]/2.$$

The results were checked using a symbolic algebra computer program available to us. The explicit matrix elements used are given in Table VIII, with $x = J(J+1)$.

Once the seven bands had been fitted separately, a modified version of the computer program was written to simultaneously fit all seven bands. This procedure is preferable to merging the results from the separate fits, particularly in a case like this, where there is a large variation in the precision of the measurements. In the separate fits the weights of the strong lines were adjusted so that the standard deviation of fit was close to one. In each case these weights were close to the expected values. The strong 0–0 and 1–1 band fits had standard deviations slightly higher than expected, probably due to the presence of small systematic lineshape distortions from ^{15}NH lines in natural abundance and unresolved hyperfine structure (*8*). Only a relatively small proportion of the lines are completely unblended and thus most of the measurements were assigned a lower weight. Deconvolution of blended lines using DECOMP was accomplished with the aid of predicted spectra, based on constants determined from the more precisely measured lines. It was possible to extract reasonably accurate positions even for multiply blended lines provided the total number of components was known, and their positions could be estimated.

The standard deviation for the global fit of all seven bands was 0.9, and there was no evidence of systematic trends in the residuals, indicating that all 1370 lines were adequately fitted. In addition to the 1240 lines measured in our Fourier transform spectrum of the $A^3\Pi$–$X^3\Sigma^-$ transition, the ground state vibrational fundamental lines of Bernath and Amano (*12*) were included. Recently the 1–0, 2–1, 3–2, and 4–3 vibrational bands of the ground state were measured by Vervloet and Brion (*16*) using a Bomem Fourier transform spectrometer. Their 1–0 and 2–1 lines were also included in the final fit, but they had little effect except for $v = 2$ due to their generally lower precision and the very large number of lines from the electronic spectrum.

Our weighted nonlinear least-squares fit of the lines in Tables I–VII with the Hamiltonian of Table VIII produced the constants of Tables IX and X. For unblended lines the weight was determined from the spectrum, while the blended lines were deweighted so that the precision was of the same order as the error (obs. − calc.) from the fit. The wavenumbers of vibration–rotation transitions of Bernath and Amano (*12*), and Vervloet and Brion (*16*) are not repeated here. These data were weighted

TABLE VIII

Matrix Elements for $^3\Pi$ and $^3\Sigma^-$ Electronic States

T[a]	(0,0)	= 1	B	(0,0)	= x+2
	(1,1)	= 1		(0,1)	= $-(2x)^{1/2}$
	(2,2)	= 1		(1,1)	= x+2
	(3,3)	= 1		(1,2)	= $-(2(x-2))^{1/2}$
	(4,4)	= 1		(2,2)	= x-2
	(5,5)	= 1		(3,3)	= x
				(3,4)	= $-2(x)^{1/2}$
A	(0,0)	= -1		(4,4)	= x+2
	(2,2)	= 1		(5,5)	= x
A_D	(0,0)	= $-(x+2)$	D	(0,0)	= $-(x^2+6x+4)$
	(0,1)	= $(x/2)^{1/2}$		(0,1)	= $2(2x)^{1/2}(x+2)$
	(1,2)	= $-(2(x-2))^{1/2}/2$		(0,2)	= $-2(x(x-2))^{1/2}$
	(2,2)	= x-2		(1,1)	= $-(x^2+8x)$
				(1,2)	= $2x(2(x-2))^{1/2}$
λ	(0,0)	= 2/3		(2,2)	= $-(x^2-2x)$
	(1,1)	= -4/3		(3,3)	= $-(x^2+4x)$
	(2,2)	= 2/3		(3,4)	= $4(x+1)(x)^{1/2}$
	(3,3)	= 2/3		(4,4)	= $-(x^2+8x+4)$
	(4,4)	= -4/3		(5,5)	= $-x^2$
	(5,5)	= 2/3			
λ_D	(0,0)	= 2(x+2)/3	γ	(0,0)	= -2
	(0,1)	= $(2x)^{1/2}/3$		(0,1)	= $(x/2)^{1/2}$
	(1,1)	= -4(x+2)/3		(1,1)	= -2
	(1,2)	= $(2(x-2))^{1/2}/3$		(1,2)	= $((x-2)/2)^{1/2}$
	(2,2)	= 2(x-2)/3		(3,3)	= -1
	(3,3)	= 2x/3		(3,4)	= $(x)^{1/2}$
	(3,4)	= $2(x)^{1/2}/3$		(4,4)	= -2
	(4,4)	= -4(x+2)/3		(5,5)	= -1
	(5,5)	= 2x/3			
o	(0,0)	= ∓ 1	γ_D	(0,0)	= -3x-4
				(0,1)	= $(2x)^{1/2}(x+6)/2$
o_D	(0,0)	= ∓(x+2)		(0,2)	= $-(x(x-2))^{1/2}$
	(0,1)	= $\pm(x/2)^{1/2}$		(1,1)	= -4x-2
				(1,2)	= $(2(x-2))^{1/2}(x+2)/2$
o_H	(0,0)	= $\mp(x^2+6x+4)$		(2,2)	= -x+2
	(0,1)	= $\pm(2x)^{1/2}(x+2)$		(3,3)	= -3x
	(0,2)	= $\mp(x(x-2))^{1/2}$		(3,4)	= $(x)^{1/2}(x+4)$
				(4,4)	= -4(x+1)
p	(0,0)	= ∓1		(5,5)	= -x
	(0,1)	= $\pm(x/2)^{1/2}$			
			γ_H	(3,3)	= $-5x^2-8x$
p_D	(0,0)	= ∓2(x+1)		(3,4)	= $(x)^{1/2}(x^2+12x+8)$
	(0,1)	= $\pm(x/2)^{1/2}(x+3)$		(4,4)	= $-6x^2-20x-8$
	(0,2)	= $\mp(x(x-2))^{1/2}/2$		(5,5)	= $-x^2$
	(1,1)	= ∓x			

Note. The upper (lower) sign refers to a state with $e(f)$ parity. Hund's case (a) basis functions were used.

[a] $(0, 0) = \langle {}^3\Pi_0|H|{}^3\Pi_0\rangle$

$0 = |{}^3\Pi_0\rangle$ $\quad 3 = |{}^3\Sigma_1^- e\rangle$ $\quad x = J(J+1)$

$1 = |{}^3\Pi_1\rangle$ $\quad 4 = |{}^3\Sigma_0^- e\rangle$

$2 = |{}^3\Pi_2\rangle$ $\quad 5 = |{}^3\Sigma_1^- f\rangle$

according to the estimated precision quoted and the quality of fit was found to be essentially the same as in the original work. A total of 78 parameters were required for the three vibrational levels of the two electronic states observed. The parameter values given in Tables IX and X have one standard deviation error estimates included. For the excited vibrational levels not all higher order parameters could be determined and thus these parameters were constrained to zero. If both A_D and γ were allowed to vary in the $A^3\Pi$ state, then a very high correlation, 0.99999, was observed between them and the values obtained did not appear realistic. For a $^2\Pi$ state it has been shown by Brown and Watson (*77*) that these two parameters cannot be simultaneously determined. However, they have both been measured in, for example, CuF (*78*) in its $b^3\Pi$ state. Clearly the problem is not a lack of data as a wide selection of rotational

TABLE VIII—*Continued*

p_H $(0,0) = \mp(3x^2+10x+4)$
$(0,1) = \pm(x/2)^{1/2}(x^2+9x+6)$
$(0,2) = \mp(x(x-2))^{1/2}(x+1)$
$(1,1) = \mp 2x(x+2)$
$(1,2) = \pm(2(x-2))^{1/2}x/2$

q $(0,0) = \mp 1$
$(0,1) = \pm(2x)^{1/2}$
$(0,2) = \mp(x(x-2))^{1/2}/2$
$(1,1) = \mp x/2$

q_D $(0,0) = \mp(3x+2)$
$(0,1) = \pm(x/2)^{1/2}(3x+4)$
$(0,2) = \mp(x(x-2))^{1/2}(x+2)/2$
$(1,1) = \mp(x+6)x/2$
$(1,2) = \pm(2(x-2))^{1/2}x/2$

q_H $(0,0) = \mp(6x^2+12x+4)$
$(0,1) = \pm(2x)^{1/2}(2x^2+8x+4)$
$(0,2) = \mp(x(x-2))^{1/2}(x^2+6x+4)/2$
$(1,1) = \mp(x^3/2+8x^2+8x)$
$(1,2) = \pm(2(x-2))^{1/2}x(x+2)$
$(2,2) = \mp x(x-2)$

q_L $(0,0) = \mp(10x^3+40x^2+36x+8)$
$(0,1) = \pm(2x)^{1/2}(5x^3/2+20x^2+28x+8)$
$(0,2) = \mp(x(x-2))^{1/2}(x^3/2+6x^2+12x+4)$
$(1,1) = \mp(x^4/2+15x^3+40x^2+16x)$
$(1,2) = \pm(2(x-2))^{1/2}(3x^3/2+8x^2+4x)$
$(2,2) = \mp(3x^3-4x^2-4x)$

H $(0,0) = x^3+12x^2+24x+8$
$(0,1) = -(2x)^{1/2}(3x^2+16x+8)$
$(0,2) = (x(x-2))^{1/2}(6x+4)$
$(1,1) = x^3+18x^2+16x$
$(1,2) = -(2(x-2))^{1/2}(3x^2+4x)$
$(2,2) = x^3-4x$
$(3,3) = x^3+12x^2+8x$
$(3,4) = -(x)^{1/2}(6x^2+20x+8)$
$(4,4) = x^3+18x^2+28x+8$
$(5,5) = x^3$

L $(0,0) = x^4+20x^3+80x^2+72x+16$
$(0,1) = -2(2x)^{1/2}(2x^3+20x^2+28x+8)$
$(0,2) = (x(x-2))^{1/2}(12x^2+24x+8)$
$(1,1) = x^4+32x^3+80x^2+32x$
$(1,2) = -2x(2(x-2))^{1/2}(2x^2+8x+4)$
$(2,2) = x^4+4x^3-8x^2-8x$
$(3,3) = x^4+24x^3+48x^2+16x$
$(3,4) = -4(x)^{1/2}(2x^3+14x^2+16x+4)$
$(4,4) = x^4+32x^3+104x^2+80x+16$
$(5,5) = x^4$

M $(0,0) = x^5+30x^4+200x^3+344x^2+192x+32$
$(0,1) = -(2x)^{1/2}(5x^4+80x^3+216x^2+160x+32)$
$(0,2) = 4(x(x-2))^{1/2}(5x^3+20x^2+18x+4)$
$(1,1) = x^5+50x^4+240x^3+256x^2+64x$
$(1,2) = -(2(x-2))^{1/2}(5x^4+40x^3+56x^2+16x)$
$(2,2) = x^5+10x^4-40x^2-16x$
$(3,3) = x^5+40x^4+160x^3+144x^2+32x$
$(3,4) = -2(x)^{1/2}(5x^4+60x^3+136x^2+88x+16)$
$(4,4) = x^5+50x^4+280x^3+416x^2+208x+32$
$(5,5) = x^5$

TABLE IX

Spectroscopic Constants (in cm^{-1}) for the $X^3\Sigma^-$ State of NH

	v = 0	v = 1	v = 2
T_v	0.0	3125.57292(25)	6094.87617(57)
B_v	16.3432784(45)	15.6964414(81)	15.050334(26)
$10^3 \times D_v$	1.702786(35)	1.679548(64)	1.65803(30)
$10^7 \times H_{Lv}$	1.23442(115)	1.17513(185)	0.9575(88)
$10^{11} \times L_v$	-1.3974(162)	-1.4396(173)	0.0
$10^{16} \times M_v$	4.18(80)	0.0	0.0
λ_v	0.920063(148)	0.921239(172)	0.91916(31)
$10^6 \times \lambda_{Dv}$	-9.09(142)	-14.67(82)	0.0
$10^2 \times \gamma_v$	-5.4844(22)	- 5.1945(31)	-4.9104(69)
$10^5 \times \gamma_{Dv}$	1.5098(75)	1.4731(117)	1.795(58)
$10^9 \times \gamma_{Hv}$	-1.366(89)	0.0	0.0

Note. One standard deviation error on the last digits is quoted in parentheses.

TABLE X

Spectroscopic Constants for the $A^3\Pi$ State of NH (in cm^{-1})

Constants	v = 0	v = 1	v = 2
T_v	29761.1829(1)	32795.9283(3)	35633.7219(6)
B_v	16.3214823(55)	15.5762834(86)	14.798763(31)
$10^3 x$ D_v	1.789698(43)	1.803235(69)	1.83399(41)
$10^7 x$ H_v	1.0739(139)	0.9390(20)	0.3278(137)
$10^{11} x$ L_v	-1.6481(197)	-3.0454(187)	0.0
$10^{15} x$ M_v	-2.757(99)	0.0	0.0
A_v	-34.61976(15)	-34.64854(33)	-34.68667(63)
$10^5 x$ A_{Dv}	-8.14[a]	-8.14[a]	-8.14[a]
λ_v	-0.19968(22)	-0.20068(27)	-0.19476(49)
$10^5 x$ λ_{Dv}	-1.630(156)	0.0	0.0
$10^2 x$ γ_v	2.9830(24)	2.8474(35)	2.8332(68)
$10^6 x$ γ_{Dv}	-5.406(52)	-3.410(133)	0.0
$10^2 x$ p_v	5.5222(25)	5.1880(41)	4.7483(103)
$10^5 x$ p_{Dv}	-1.7795(151)	-1.979(31)	-2.358(135)
$10^9 x$ p_{Hv}	2.124(193)	1.61(59)	0.0
$10^2 x$ q_v	-3.15870(40)	-2.95597(33)	-2.73942(121)
$10^5 x$ q_{Dv}	1.3822(29)	1.3879(20)	1.5275(114)
$10^9 x$ q_{Hv}	-1.861(66)	-1.086(32)	0.0
$10^{13} x$ q_{Lv}	1.95(46)	0.0	0.0
o_v	1.28447(20)	1.22637(26)	1.15014(56)
$10^4 x$ o_{Dv}	-1.3440(136)	-1.703(31)	-2.072(99)
$10^8 x$ o_{Hv}	-3.07(24)	-6.30(71)	0.0

Note. One standard deviation uncertainties in parentheses.
[a] Fixed at computed value (see text for details).

levels in both Λ doublets of all three spin–orbit components have been measured. Veseth (*79*) provides a formula relating A_D to other constants:

$$A_D = 2A_J = \frac{2(A_{v+1} - A_v)D_{v=0}}{B_v - B_{v+1} + 6B_e^2/\omega_e}.$$

For $v = 0$ this gives $A_D = -8.14 \times 10^{-5}$ cm^{-1}. For the final fit, A_D was constrained to this value for all three vibrational levels.

The term values for the first three vibrational levels of the $A^3\Pi$ and $X^3\Sigma^-$ states of NH have been calculated (for the range of rotational levels studied in each case) and are given in Table XI. Any unmeasured lines can be determined from these term values. The term values have been extrapolated only to slightly higher J than was observed in the spectrum. The large number of high-order distortion constants required in the fit means that significant errors will soon occur in any extrapolation.

IV. DISCUSSION

Relative Intensities

Emission from $v = 0$, 1, and 2 in the $A^3\Pi$ state of NH was observed. The 0–0 and 1–1 bands appear to differ in intensity by about a factor of 2 while the 2–2 band is an order of magnitude weaker. This is shown clearly in Fig. 1. The relative transition probabilities of the three bands are approximately equal (*50*) and thus a purely Boltzmann distribution of vibrational energy would imply a decrease of about a factor of 4 for the 2–2 band relative to the 0–0. Smith *et al.* (*52*) have measured the variation in lifetime with rotational quantum number for $v = 0$ and $v = 1$ of the $A^3\Pi$ state of NH. They observe predissociation in the $v = 0$ level beginning at $N = 24$ and in $v = 1$ from $N = 13$ onward. They find that the perturbing state, thought to be of $^5\Sigma^-$ symmetry, crosses the $A^3\Pi$ potential curve at 34 000 cm^{-1}. This is below the first rotational level for $v = 2$, implying that all $v = 2$ levels are predissociated. The shortening of the lifetime leads to fewer molecules fluorescing and hence a weaker band. Relative intensities for the 0–0, 1–1, and 2–2 bands at low and intermediate N have been measured from the spectrum and are given in Table XII. The ratio of $v = 0$ to $v = 1$ intensity indicates a vibrational temperature of 5400 K. This predicts an intensity for the 2–2 band of 0.21, relative to 0–0, in the absence of predissociation. Other bands such as 3–3 and 4–4 would also be easily observable if there was no predissociation. The decrease in relative 2–2 band intensity at low N from the expected 0.21 to the observed 0.068 implies a predissociation lifetime of 200 nsec, assuming a fluorescent lifetime of 410 nsec (*50, 52*). The overall lifetime is thus 130 nsec, for $N = 3$ or 4 of $A^3\Pi$, $v = 2$. At $N = 13$ for $v = 2$, the decrease is much greater, implying a predissociation lifetime of 50 nsec and an overall lifetime of 45 nsec. The lines decrease rapidly in intensity with increasing N, and are unobservable beyond $N = 18$, indicating essentially complete predissociation.

Equilibrium Constants

From the molecular constants for $v = 0$, 1, and 2 of $A^3\Pi$ and $X^3\Sigma^-$ reported in Tables IX and X, equilibrium constants were determined (Table XIII). For the vibrational constants only $\Delta G_{1/2}$ and $\Delta G_{3/2}$ are available so two constants, ω_e and $\omega_e x_e$, could be determined. The neglect of $\omega_e y_e$ introduces a large error into our estimated vibrational constants in Table XIII [$\omega_e y_e$ is 0.33 cm^{-1} for $X^3\Sigma^-$ (*16*)]. Our values for $\Delta G''_{1/2}$ and $\Delta G''_{3/2}$ agree with previous determinations (*12, 16*).

Equilibrium values for the fine structure and rotational constants may also be derived. The spin–orbit constant, A, was fitted to a linear expression in $(v + 1/2)$ because, although the deviation from linearity is much greater than the random error, there is a possibility of small systematic deviations. The spin splitting constant λ for both the ground and excited states shows no clear variation with v.

An exact fit to three parameters B_e, α_e, and γ_e was made for the rotational constants of both states. The errors quoted in Table XIII were computed by the customary rules for error propagation, the true error is probably an order of magnitude larger than this. The equilibrium bond length r_e was then calculated and the values obtained are consistent with, but much more accurate than, the previous values.

TABLE XI

Term Energies (in cm^{-1})

$X^3\Sigma^-$

	v=0			v=1			v=2		
J	F_1	F_2	F_3	F_1	F_2	F_3	F_1	F_2	F_3
0			31.5626			3155.8346			6123.8428
1	-0.0077	33.3479	97.5570	3125.5649	3157.6251	3219.2407	6094.8678	6125.6321	6184.6611
2	32.4973	98.6665	195.6073	3156.7791	3220.3571	3313.4096	6124.7932	6185.7803	6274.9523
3	97.7100	196.5423	326.0237	3219.4082	3314.3544	3438.6544	6184.8415	6275.9033	6395.0304
4	195.5031	326.8532	488.6896	3313.3256	3439.4965	3594.8605	6274.8876	6395.8819	6544.7825
5	325.7419	489.4368	683.4147	3438.3986	3595.6231	3781.8406	6394.8001	6545.5579	6724.0236
6	488.2594	684.0904	909.9620	3594.4620	3782.5345	3999.3605	6544.4159	6724.7337	6932.5220
7	682.8508	910.5722	1168.0523	3781.3141	3999.9918	4247.1451	6723.5354	6933.1730	7170.0053
8	909.2732	1168.6012	1457.3676	3998.7150	4247.7177	4524.8801	6931.9214	7170.6013	7436.1621
9	1167.2449	1457.8579	1777.5510	4246.3866	4525.3969	4832.2133	7169.2988	7436.7063	7730.6434
10	1456.4462	1777.9851	2128.2088	4524.0133	4832.6767	5168.7557	7435.3546	7731.1381	8053.0630
11	1776.5196	2128.5885	2508.9106	4831.2422	5169.1675	5534.0822	7729.7393	8053.5105	8402.9989
12	2127.0709	2509.2378	2919.1907	5167.6839	5534.4442	5927.7324	8052.0662	8403.4011	8779.9934
13	2507.6694	2919.4669	3358.5487	5532.9128	5928.0462	6349.2116	8401.9129	8780.3523	9183.5547
14	2917.8493	3358.7756	3826.4509	5926.4686	6349.4788	6797.9916	8778.8221	9183.8721	9613.1572
15	3357.1102	3826.6300	4322.3307	6347.8566	6798.2139	7273.5118	9182.3016	9613.4351	10068.2429
16	3824.9183	4322.4636	4845.5902	6796.5485	7273.6907	7775.1800	9611.8261	10068.4832	10548.2223
17	4320.7072	4845.6785	5395.6011	7271.9839	7775.3173	8302.3735	10066.8377	10548.4270	11052.4753
18	4843.8790	5395.6464	5971.7054	7773.5707	8302.4707	8854.4397	10546.7469	11052.6465	11580.3528
19	5393.8052	5971.7093	6573.2171	8300.6860	8854.4987	9430.6976	11050.9338	11580.4926	12131.1776
20	5969.8283	6573.1813	7199.4227	8852.6777	9430.7202	10030.4383	11578.7495	12131.2882	12704.2457
21	6571.2621	7199.3488	7849.5826	9428.8648	10030.4264	10652.9263	12129.5168	12704.3295	13298.8280
22	7197.3932	7849.4725	8522.9320	10028.5386	10652.8818	11297.3998			
23	7847.4821	8522.7875	9218.6823	10650.9635	11297.3249	11963.0724			
24	8520.7643	9218.5051	9936.0213	11295.3783	11962.9690	12649.1328			
25	9216.4509	9935.8133	10674.1148	11960.9962	12649.0033	13354.7466			
26	9933.7301	10673.8780	11432.1075	12647.0066	13354.5931	14079.0559			
27	10671.7676	11431.8437	12209.1232	13352.5748	14078.8808	14821.1806			
28	11429.7081	12208.8343	13004.2661	14076.8435	14820.9863	15580.2181			
29	12206.6756	13003.9542	13816.6214	14818.9323	15580.0072	16355.2442			
30	13001.7743	13816.2884	14645.2553	15577.9392	16355.0193	17145.3127			
31	13814.0893	14644.9033	15489.2164						
32	14642.6870	15488.8473	16347.5349						
33	15486.6159	16347.1507	17219.2238						
34	16344.9064	17218.8266	18103.2782						

$A^3\Pi$ e levels

	v=0			v=1			v=2		
J	F_1	F_2	F_3	F_1	F_2	F_3	F_1	F_2	F_3
0			29826.9380			32860.2833			35696.6427
1		29806.6075	29879.6166		32839.7212	32910.1239		35675.7942	35743.5279
2	29770.6137	29866.0956	29971.6086	32803.6533	32896.4276	32997.6256	35639.6505	35729.6159	35826.3374
3	29842.3149	29960.6994	30098.4773	32872.3573	32986.5989	33118.4991	35705.2232	35815.1692	35940.9456
4	29943.9814	30089.0510	30258.7572	32969.5683	33108.9896	33271.2906	35797.7849	35931.3388	36085.9101
5	30076.7147	30250.2736	30451.7101	33096.3532	33262.7538	33455.2614	35918.3614	36077.3130	36260.4886
6	30240.9288	30443.8228	30676.8267	33253.1186	33447.3520	33669.8994	36067.3480	36252.5560	36464.1621
7	30436.7067	30669.2850	30933.6725	33439.9453	33662.3691	33914.7662	36244.8206	36456.6484	36696.4836
8	30663.9548	30926.2832	31221.8284	33656.7382	33907.4249	34189.4386	36450.6789	36689.2025	36957.0196
9	30922.4704	31214.4369	31540.8652	33903.2929	34182.1352	34493.4825	36684.7116	36949.8245	37245.3237
10	31211.9740	31533.3443	31890.3314	34179.3267	34486.0933	34826.4404	36946.6273	37238.0961	37560.9243
11	31532.1249	31882.5742	32269.7466	34484.4949	34818.8624	35187.8253	37236.0704	37553.5669	37903.3174
12	31882.5300	32261.6620	32678.5985	34818.3996	35179.9716	35577.1170	37552.6294	37895.7497	38271.9631
13	32262.7495	32670.1086	33116.3418	35180.5948	35568.9138	35993.7601	37895.8419	38264.1185	38666.2837
14	32672.2999	33107.3791	33582.3968	35570.5891	35985.1447	36437.1635	38265.1977	38658.1075	39085.6626
15	33110.6567	33572.9036	34076.1496	35987.8487	36428.0830	36906.6995	38660.1408	39077.1107	39529.4434
16	33577.2557	34066.0766	34596.9524	36431.7983	36897.1098	37401.7039	39080.0705	39520.4816	39996.9301
17	34071.4952	34586.2580	35144.1236	36901.8221	37391.5689	37921.4752	39524.3428	39987.5334	40487.3866
18	34592.7363	35132.7734	35716.9480	37397.2651	37910.7667	38465.2752	39992.2711	40477.5389	41000.0373
19	35140.3045	35704.9148	36314.6777	37917.4334	38453.9724	39032.3283	40483.1268	40989.7313	41534.0669
20	35713.4904	36301.9408	36936.5319	38461.5943	39020.4175	39621.8216	40996.1401	41523.3040	42088.6209
21	36311.5507	36923.0772	37581.6976	39028.9770	39609.2962	40232.9042	41530.5003	42077.4113	42662.8059
22	36933.7083	37567.5172	38249.3297	39618.7723	40219.7646	40864.6869			
23	37579.1532	38234.4221	38938.5508	40230.1324	40850.9404	41516.2413			
24	38247.0427	38922.9206	39648.4514	40862.1705	41501.9021	42186.5988			
25	38936.5017	39632.1092	40378.0892	41513.9604	42171.6881	42874.7496			
26	39646.6222	40361.0518	41126.4888	42184.5353	42859.2954	43579.6409			
27	40376.4635	41108.7788	41892.6403	42872.8868	43563.6781	44300.1752			
28	41125.0514	41874.2865	42675.4984	43577.9634	44283.7455	45035.2080			
29	41891.3770	42656.5354	43473.9807	44298.6684	45018.3599	45783.5451			
30	42674.3961	43454.4488	44286.9651	45033.8584	45766.3341	46543.9400			
31	43473.0268	44266.9104	45113.2874						
32	44286.1478	45092.7619	45951.7378						
33	45112.5954	45930.7992	46801.0574						
34	45951.1605	46779.7689	47659.9328						

The centrifugal distortion terms D and H were each fitted to two parameters using a weighted least-squares fit of the three available points. The results obtained for D_e and H_e can be compared with those calculated from the Kratzer and Dunham-Birge

TABLE XI—*Continued*

$A^3\Pi$ f levels

	v=0			v=1			v=2		
J	F_1	F_2	F_3	F_1	F_2	F_3	F_1	F_2	F_3
0			29829.5537			32862.7800			35698.9823
1		29807.2753	29881.5009		32840.3364	32911.9456		35676.3484	35745.2578
2	29770.6018	29867.1478	29972.9936	32803.6415	32897.4104	32998.9727	35639.6386	35730.5162	35827.6226
3	29842.2289	29962.0323	30099.4665	32872.2766	32987.8499	33119.4691	35705.1480	35816.3228	35941.8759
4	29943.7378	30090.6696	30259.3672	32969.3417	33110.5105	33271.9013	35797.5762	35932.7445	36086.5034
5	30076.2322	30252.2176	30451.9227	33095.9048	33264.5799	33455.4972	35917.9496	36079.0016	36260.7322
6	30240.1323	30446.1419	30676.6084	33252.3782	33449.5287	33669.7301	36066.6687	36254.5681	36464.0297
7	30435.5274	30672.0313	30932.9833	33438.8487	33664.9442	33914.1554	36243.8152	36459.0266	36695.9434
8	30662.3289	30929.5086	31220.6256	33655.2261	33910.4461	34188.3475	36449.2938	36691.9890	36956.0378
9	30920.3387	31218.1915	31539.1061	33901.3105	34185.6481	34491.8723	36682.8977	36953.0592	37243.8673
10	31209.2814	31537.6758	31887.9741	34176.8232	34490.1413	34824.2734	36944.3400	37241.8163	37558.9615
11	31528.8202	31887.5275	32266.7514	34481.4237	34823.4859	35185.0659	37233.2694	37557.8065	37900.8194
12	31878.5660	32267.2787	32674.9283	34814.7180	35185.2076	35573.7324	37549.2789	37900.5385	38268.9044
13	32258.0829	32676.4268	33111.9626	35176.2641	35574.7954	35989.7209	37891.9109	38269.4823	38662.6430
14	32666.8915	33114.4331	33577.2780	35565.5751	35991.7014	36432.4441	38260.6599	38664.0672	39081.4229
15	33104.4716	33580.7237	34070.2647	35982.1214	36435.3397	36901.2783	38654.9752	39083.6821	39524.5930
16	33570.2634	34074.6887	34590.2788	36425.3323	36905.0871	37395.5636	39074.2617	39527.6752	39991.4625
17	34063.6696	34595.6838	35136.6431	36894.5971	37400.2824	37914.6034	39517.8810	39995.3536	40481.3015
18	34584.0560	35143.0298	35708.6471	37389.2656	37920.2270	38457.6645	39985.1527	40485.9842	40993.3404
19	35130.7530	35716.0139	36305.5474	37908.6492	38464.1849	39023.9765	40475.3548	40998.7934	41526.7708
20	35703.0562	36313.8898	36926.5683	38452.0205	39031.3821	39612.7317	40987.7241	41532.9678	42080.7452
21	36300.2272	36935.8782	37570.9018	39018.6144	39621.0072	40223.0851	41521.4573	42087.6543	42654.3777
22	36921.4941	37581.1672	38237.7078	39607.6274	40232.2105	40854.1531			
23	37566.0523	38248.9127	38926.1142	40218.2175	40864.1038	41505.0133			
24	38233.0643	38938.2381	39635.2169	40849.5041	41515.7593	42174.7032			
25	38921.6604	39648.2347	40364.0788	41500.5671	42186.2094	42862.2190			
26	39630.9381	40377.9606	41111.7299	42170.4460	42874.4446	43566.5144			
27	40359.9623	41126.4409	41877.1660	42858.1386	43579.4127	44286.4980			
28	41107.7641	41892.6663	42659.3471	43562.5999	44300.0164	45021.0317			
29	41873.3403	42675.5919	43457.1963	44282.7399	45035.1117	45768.9279			
30	42655.6521	43474.1352	44269.5969	45017.4214	45783.5048	46528.9463			
31	43453.6232	44287.1747	45095.3903						
32	44266.1378	45113.5462	45933.3723						
33	45092.0377	45952.0404	46782.2892						
34	45930.1192	46801.3982	47640.8334						

relations (*73*), respectively (Table XIII). In all four cases the experimental and calculated values are in good agreement.

Λ-*Doubling and Spin–Rotation Interactions*

The Λ-doubling and spin–rotation constants can be calculated assuming pure precession (*80*) between the $A^3\Pi$ and $X^3\Sigma^-$ states. Contributions to p, q, and γ arise only from triplet states, of which $A^3\Pi$ and $X^3\Sigma^-$ are the only two known. Theoretical calculations by Kouba and Öhrn (*57*) predict weakly bound $^3\Pi$ and $^3\Sigma^-$ states near the $A^3\Pi$ state, but due to the large difference in equilibrium bond lengths, the Franck-Condon factors are likely to be small. There may also be high-lying Rydberg states, but these will have comparatively little effect due to the large energy separation. In the case of pure precession between a $^3\Sigma^-$ and a $^3\Pi$ state the value of γ in the $^3\Sigma^-$

TABLE XII

Relative Intensities for Selected Lines of the $A^3\Pi$–$X^3\Sigma^-$ Transition of NH

Lines $P_F(N)$	v=0	v=1	v=2
$P_2(4)$	251	112	17
$P_1(5)$	355	158	24
$P_2(13)$	220	89	4.8
$P_1(14)$	240	100	5.2

TABLE XIII

Equilibrium Constants for $A^3\Pi$ and $X^3\Sigma^-$ States of NH (in cm^{-1})

Constant	$A^3\Pi$	$X^3\Sigma^-$
$\Delta G_{1/2}$	3034.7454(3)	3125.5729(3)
$\Delta G_{3/2}$	2837.7937(7)	2969.3033(6)
ω_e	3232(2)	3281(2)
$\omega_e x_e$	98(1)	78(1)
B_e	16.681963(8)	16.666970(7)
α_e	0.712880(35)	0.647567(31)
γ_e	-0.016160(24)	0.000365(20)
$10^4 x D_e$	17.822(28)	17.1431(31)
$10^4 x \beta_e$	0.146(31)	-0.2309(36)
$10^4 x D_e$	17.781[a]	17.195[a]
A_e	-34.6038(23)	---
α_A	- 0.0314(26)	---
$10^8 x H_e$	11.6(8)	12.7(3)
$10^8 x \alpha_H$	- 1.6(8)	-0.7(3)
$10^8 x H_e$	11.8[b]	12.8[b]
r_e	1.03675A	1.03722A

Note. Estimated one standard deviation error in parentheses.

[a] Computed using the Kratzer relationship.

[b] Computed using the Dunham–Birge expression.

state is equal and opposite in sign to p for the $^3\Pi$ state. For NH in the $v = 0$ levels the values are $\gamma^\Sigma = -0.0548$ and $p^\Pi = 0.0552$.

Expressions for o, p, and q in terms of matrix elements connecting electronic states are given by Brown and Merer (*76*) [Refs. (*81, 82*) are also helpful]. The ground state of NH has a $1\sigma^2 2\sigma^2 3\sigma^2 1\pi^2$ configuration and the $A^3\Pi$ state is $1\sigma^2 2\sigma^2 3\sigma^1 1\pi^3$. In order to evaluate the interaction matrix elements a total of four electrons in 3σ and 1π orbitals must be considered. The matrix elements can be evaluated if 3σ and 1π are considered to be nitrogen atomic $2p_z$ and $2p_{\pm 1}$ orbitals, respectively. The Slater determinant representations of the $^3\Pi$ and $^3\Sigma^-$ components are given in Table XIV. The required matrix elements were evaluated using the determinants of Table XIV and the pure precession hypothesis (*80*) with $l = 1$. The results are

$$p = 2\zeta B/(E_\Pi - E_\Sigma) = -4AB/(E_\Pi - E_\Sigma)$$

$$q = -4B^2/(E_\Pi - E_\Sigma)$$

where ζ is the atomic spin–orbit coupling parameter as defined by Tinkham (*83*). The molecular and atomic spin–orbit parameters are related by $A = -\zeta/2$. As a test of the pure precession hypothesis, the atomic $\zeta = 73.3$ cm^{-1} (*84*) results in a predicted A of -36.6 cm^{-1} compared to the observed $A_0 = -34.6$ cm^{-1}. The pure precession p_0 and q_0 values are 0.0759 and -0.0358 cm^{-1} compared to the observed 0.0552 and -0.0316

TABLE XIV

Slater Determinant Representation of the Electronic Structure of $A^3\Pi$ and $X^3\Sigma^-$ States of NH

$\|^3\pi_2\rangle$ =	$1/\sqrt{2}\ (\|\sigma\pi_+\ \bar{\pi}_+\ \pi_-\ \|\mp\|\ \bar{\sigma}\ \bar{\pi}_+\pi_-\bar{\pi}_-\|)$
$\|^3\pi_1\rangle$ =	$1/2\ ((\|\bar{\sigma}\pi_+\bar{\pi}_+\pi_-\|+\|\sigma\pi_+\bar{\pi}_+\bar{\pi}_-\|)\mp(\|\bar{\sigma}\pi_+\pi_-\bar{\pi}_-\|+\|\sigma\bar{\pi}_+\pi_-\bar{\pi}_-\|))$
$\|^3\pi_0\rangle$ =	$1/\sqrt{2}\ (\|\bar{\sigma}\pi_+\bar{\pi}_+\pi_-\|+\|\sigma\pi_+\pi_-\bar{\pi}_-\|)$
$\|^3\Sigma^-_1\rangle$ =	$1/\sqrt{2}\ (\|\sigma\bar{\sigma}\ \pi_+\pi_-\|\mp\|\sigma\bar{\sigma}\ \bar{\pi}_+\bar{\pi}_-\|)$
$\|^3\Sigma^-_0 e\rangle$ =	$1/\sqrt{2}\ (\|\sigma\bar{\sigma}\ \bar{\pi}_+\pi_-\|+\|\sigma\bar{\sigma}\pi_+\bar{\pi}_-\|)$

Note. The upper (lower) sign refers to $e(f)$ parity.

cm^{-1}, respectively. The agreement for A and q is very good but p is predicted much more poorly. Considering that only two well-separated electronic states were considered, Franck-Condon factors were taken as $\delta_{vv'}$ and the extreme nature of the basic pure precession assumption of $l = 1$, the overall agreement is satisfactory.

For a $^3\Pi$ state interacting with a single $^3\Sigma^-$ state, the spin–rotation and Λ-doubling parameters are related by $\gamma^{\Pi} \approx p^{\Pi}/2$ (*76*). The NH $A^3\Pi$ state has $p_0/2 = 0.0276\ cm^{-1}$ compared with the observed $0.0297\ cm^{-1}$. This relationship neglects interactions with other electronic states ($^3\Delta$ affects γ but not p) and first-order contributions to γ (the "true" spin–rotation interaction). Also since A_D and γ are badly correlated, our assumed value of A_D also affects γ.

There is an additional Λ-doubling parameter for a $^3\Pi$ state, o. This contains a first-order contribution from the spin–spin interaction as well as second-order effects through spin–orbit coupling. Horani *et al.* (*85*) have investigated this for a series of molecules isovalent with NH. For those species where the spin–orbit interaction is large the second-order effects dominate, while for cases like NH where A is small the spin–spin interaction is most important. They calculated the spin–spin contribution to be 1.4 cm^{-1} with small negative terms from the spin–orbit interaction, bringing the value close to the measured one.

The first centrifugal distortion correction to the Λ-doubling p_D and q_D can be estimated using the formulae due to Veseth (*79*):

$$p_D = 2p\left(\frac{A_D}{A} - \frac{D}{B}\right)$$

$$q_D = -4q\left(\frac{D}{B}\right).$$

A_D was not determined but the calculated value gives a negligible contribution. From the equations the calculated values for $v = 0$ are

$$p_D = -1.2 \times 10^{-5} \qquad \text{cf. } -1.8 \times 10^{-5}$$

$$q_D = 1.39 \times 10^{-5} \qquad \text{cf. } 1.38 \times 10^{-5}.$$

The agreement for p_D is reasonable while the value for q_D is so close that the agreement must be considered fortuitous.

The correction to the spin–rotation interaction can also be estimated using the equivalent formula from Veseth (*79*):

$$\gamma_D = 2\gamma\left(\frac{A_D}{A} - \frac{D}{B}\right).$$

Again neglecting the first term, the following result is obtained:

$$\gamma_D = -6.5 \times 10^{-5} \qquad \text{cf. } -5.4 \times 10^{-5}.$$

CONCLUSION

The $A^3\Pi$–$X^3\Sigma^-$ transition of NH has been analyzed with much higher precision than in previous work. A total of seven vibrational bands were simultaneously fitted yielding 78 molecular constants. The improved data should prove useful to the many workers studying the NH molecule.

ACKNOWLEDGMENTS

We are grateful for the expert technical assistance of Rob Hubbard in acquiring the NH spectrum. We thank Jim Brault for the helium spectra employed to calibrate our data, and his interest in this work. This work was supported by funding from the Office of Naval Research (N00014-84-K-0122).

RECEIVED: April 3, 1986

REFERENCES

1. J. M. EDER, *Denksch. Wien. Akad.* **60,** 1 (1893).
2. G. FUNKE, *Z. Phys.* **96,** 787–798 (1935); **101,** 104–112 (1936).
3. R. N. DIXON, *Canad. J. Phys.* **37,** 1171–1186 (1959).
4. T. MURAI AND M. SHIMAUCHI, *Sci. Light (Tokyo)* **15,** 48–67 (1966).
5. J. MALICET, J. BRION, AND H. GUENEBAUT, *J. Chim. Phys.* **67,** 25–30 (1970).
6. M. SHIMAUCHI, *Sci. Light (Tokyo)* **15,** 161–165 (1966); **16,** 185–190 (1967).
7. P. BOLLMARK, I. KOPP, AND B. RYDH, *J. Mol. Spectrosc.* **34,** 487–499 (1970).
8. W. UBACHS, J. J. TER MEULEN, AND A. DYMANUS, *Canad. J. Phys.* **62,** 1374–1385 (1984).
9. H. E. RADFORD AND M. M. LITVAK, *Chem. Phys. Lett.* **34,** 561–564 (1975).
10. F. D. WAYNE AND H. E. RADFORD, *Mol. Phys.* **32,** 1407–1422 (1976).
11. F. C. VAN DER HEUVEL, W. L. MEERTS, AND A. DYMANUS, *Chem. Phys. Lett.* **92,** 215–218 (1982).
12. P. F. BERNATH AND T. AMANO, *J. Mol. Spectrosc.* **95,** 359–364 (1982).
13. D. E. MILLIGAN AND M. E. JACOX, *J. Chem. Phys.* **41,** 2838–2841 (1964).
14. H. SAKAI, P. HANSEN, M. ESPLIN, R. JOHANSSON, M. PELTOLA, AND J. STRONG, *Appl. Opt.* **21,** 228–234 (1982).
15. B. D. GREEN AND G. E. CALEDONIA, *J. Chem. Phys.* **77,** 3821–3823 (1982).
16. M. VERVLOET AND J. BRION, personal communication.
17. D. BOUDJAADAR, P. CHOLLET, AND G. GUELACHVILI, Fortieth Symposium on Molecular Spectroscopy, June, 1985, Columbus, Ohio.
18. R. W. B. PEARSE, *Proc. R. Soc. London, Ser. A* **143,** 112–123 (1933).
19. G. H. DIEKE AND R. W. BLUE, *Phys. Rev.* **45,** 395–400 (1934).
20. G. NAKAMURA AND T. SHIDEI, *Japan. J. Phys.* **10,** 5–10 (1935).
21. W. Y. CHEUNG, B. GELERNT, AND T. CARRINGTON, *Chem. Phys. Lett.* **66,** 287–290 (1979).

22. D. RAMSAY AND P. SARRE, *J. Mol. Spectrosc.* **93,** 445–446 (1982).
23. W. UBACHS, G. MEYER, J. J. TER MEULEN, AND A. DYMANUS, *J. Mol. Spectrosc.* **115,** 88–104 (1986).
24. R. S. RAM AND P. F. BERNATH, *J. Opt. Soc. Amer. Opt. Phys. B.* **3,** 1170–1174 (1986).
25. R. W. LUNT, R. W. B. PEARSE, AND E. C. W. SMITH, *Proc. R. Soc. London, Ser. A* **151,** 602–609 (1935).
26. F. L. WHITTAKER, *J. Phys. B.* **1,** 977–982 (1968).
27. R. W. LUNT, R. W. B. PEARSE, AND E. C. W. SMITH, *Proc. R. Soc. London, Ser. A* **155,** 173–182 (1936).
28. F. L. WHITTAKER, *Proc. Phys. Soc. London* **90,** 535–541 (1967).
29. G. KRISHNAMURTY AND W. A. NARASIMHAM, *J. Mol. Spectrosc.* **29,** 410–414 (1969); *Proc. Indian Acad. Sci., Sect. A* **64,** 97–110 (1966).
30. W. R. M. GRAHAM AND H. LEW, *Canad. J. Phys.* **56,** 85–99 (1978).
31. J. L. HALL, H. ADAMS, J. V. V. KASPER, R. F. CURL, AND F. K. TITTEL, *J. Opt. Soc. Amer. Opt. Phys. B:* **2,** 781–785 (1985).
32. K. R. LEOPOLD, K. M. EVENSON, AND J. M. BROWN, *J. Chem. Phys.* **85,** 324–330 (1986).
33. J. MASANET, A. GILLES, AND C. VERMEIL, *J. Photochem.* **3,** 417–429 (1974).
34. P. C. ENGELKING AND W. C. LINEBERGER, *J. Chem. Phys.* **65,** 4323–4324 (1976).
35. D. COSSART, *J. Chim. Phys.* **76,** 1045–1050 (1979).
36. F. ROHRER AND F. STUHL, *Chem. Phys. Lett.* **111,** 234–237 (1984).
37. A. HOFZUMAHAUS AND F. STUHL, *J. Chem. Phys.* **82,** 3152–3159 (1985); **82,** 5519–5526 (1985); H. HAAK AND F. STUHL, *J. Phys. Chem.* **88,** 3627–3633; **88,** 2201–2204 (1984); U. BLUMENSTEIN, F. ROHRER, AND F. STUHL, *Chem. Phys. Lett.* **107,** 347–350 (1984).
38. B. GELERNT, S. V. FILSETH, AND T. CARRINGTON, *Chem. Phys. Lett.* **36,** 238–241 (1975).
39. J. MASANET, C. LALO, G. DURAND, AND C. VERMEIL, *Chem. Phys.* **33,** 123–130 (1978).
40. Y. MARUYAMA, T. HIKIDA, AND Y. MORI, *Chem. Phys. Lett.* **116,** 371–373 (1985).
41. F. ALBERTI AND A. DOUGLAS, *Chem. Phys.* **34,** 399–402 (1978).
42. E. N. TERESHCHENKO AND N. YA. DODONOVA, *Opt. Spectrosc.* **47,** 339–340 (1979).
43. A. M. QUINTON AND J. P. SIMONS, *Chem. Phys. Lett.* **81,** 214–217 (1981).
44. N. WASHIDA, G. INOUE, M. SUZUKI, AND O. KAJIMOTO, *Chem. Phys. Lett.* **114,** 274–278 (1985).
45. C. HELLNER, K. T. V. GRATTAN, AND M. H. R. HUTCHINSON, *J. Chem. Phys.* **81,** 4389–4395 (1984).
46. I. TOKUE AND Y. ITO, *Chem. Phys.* **79,** 383–389 (1983); **89,** 51–57 (1984); I. TOKUE AND M. IWAI, *Chem. Phys.* **52,** 47–53 (1980).
47. P. G. CARRICK AND P. C. ENGELKING, *Chem. Phys. Lett.* **108,** 505–508 (1984).
48. J. M. LENTS, *J. Quant. Spectrosc. Radiat. Transfer* **13,** 297–310 (1973).
49. J. A. HARRINGTON, A. P. MODICA, AND D. R. LIBBY, *J. Quant. Spectrosc. Radiat. Transfer* **6,** 799–805 (1966).
50. P. W. FAIRCHILD, G. P. SMITH, D. R. CROSLEY, AND J. B. JEFFRIES, *Chem. Phys. Lett.* **107,** 181–186 (1984).
51. N. L. GARLAND, J. B. JEFFRIES, D. R. CROSLEY, G. P. SMITH, AND R. A. COPELAND, *J. Chem. Phys.* **85,** 4970–4975 (1986).
52. W. H. SMITH, J. BRZOZOWSKI, AND P. ERMAN, *J. Chem. Phys.* **64,** 4628 (1976).
53. L. ZETZSCH, *Ber. Bunsenges. Phys. Chem.* **82,** 639–643 (1978).
54. S. N. FONER AND R. L. HUDSON, *J. Chem. Phys.* **74,** 5017–5021 (1981).
55. E. A. SCARL AND F. W. DALBY, *Canad. J. Phys.* **52,** 1429–1437 (1974).
56. S. T. GIBSON, J. P. GREENE, AND J. BERKOWITZ, *J. Chem. Phys.* **83,** 4319–4328 (1985).
57. J. KOUBA AND Y. ÖHRN, *J. Chem. Phys.* **52,** 5387–5394 (1970).
58. P. J. HAY AND T. H. DUNNING, JR., *J. Chem. Phys.* **64,** 5077–5087 (1976).
59. W. MEYER AND P. ROSMUS, *J. Chem. Phys.* **63,** 2356–2375 (1975).
60. B. S. HAYNES, *Combust. Flame* **28,** 81–91 (1977).
61. J. A. MILLER, *Combust. Flame* **43,** 81–98 (1981).
62. W. R. ANDERSON, L. J. DECKER, AND A. J. KOTLAR, *Combust. Flame* **48,** 179–190 (1982).
63. M. S. CHOU, A. M. DEAN, AND D. STERN, *J. Chem. Phys.* **76,** 5334–5340 (1982).
64. A. FOWLER AND C. C. L. GREGORY, *Philos. Trans. R. Soc. London, Ser. A* **218,** 351–372 (1919).
65. R. W. SHAW, *Astrophys. J.* **83,** 225–237 (1936).
66. J. L. SCHMITT, *Publ. Astron. Soc. Pac.* **81,** 657–664 (1969).
67. P. SWINGS, C. T. ELVEY, AND H. W. BABCOCK, *Astrophys. J.* **94,** 320–343 (1941).
68. M. M. LITVAK AND E. N. R. KUIPER, *Astrophys. J.* **253,** 622–633 (1982).

69. D. L. LAMBERT, J. A. BROWN, K. H. HINKLE, AND H. R. JOHNSON, *Astrophys. J.* **284,** 223–237 (1984).
70. S. T. RIDGWAY, D. F. CARBON, D. N. B. HALL, AND J. JEWELL, *Astrophys. J. Suppl.* **54,** 177–210 (1984).
71. W. C. MARTIN, *J. Res. Nat. Bur. Stand., Sect. A* **64,** 19–28 (1960).
72. G. NORLEN, *Physica Scripta* **8,** 249–268 (1973).
73. G. HERZBERG, "Spectra of Diatomic Molecules," 2nd ed., Van Nostrand–Reinhold, New York, 1950.
74. R. N. ZARE, A. L. SCHMELTEKOPF, W. J. HARROP, AND D. L. ALBRITTON, *J. Mol. Spectrosc.* **46,** 37–66 (1973).
75. F. ROUX, D. CERNY, AND J. VERGES, *J. Mol. Spectrosc.* **94,** 302–308 (1982).
76. J. M. BROWN AND A. J. MERER, *J. Mol. Spectrosc.* **74,** 488–494 (1979).
77. J. M. BROWN AND J. K. G. WATSON, *J. Mol. Spectrosc.* **65,** 65–74 (1977).
78. T. C. STEIMLE, C. R. BRAZIER, AND J. M. BROWN, *J. Mol. Spectrosc.* **110,** 39–52 (1985).
79. L. VESETH, *J. Phys. B* **3,** 1677–1691 (1970).
80. R. S. MULLIKEN AND A. CHRISTY, *Phys. Rev.* **38,** 87–119 (1931).
81. A. J. MERER, D. N. MALM, R. W. MARTIN, M. HORANI, AND J. ROSTAS, *Canad. J. Phys.* **53,** 251–283 (1975).
82. B. G. WICKE, R. W. FIELD, AND W. KLEMPERER, *J. Chem. Phys.* **56,** 5758–5770 (1972).
83. M. TINKHAM, "Group Theory and Quantum Mechanics," McGraw–Hill, New York, 1964.
84. C. E. MOORE, "Atomic Energy Levels," Vol. 1, NSRDS-NBS 35, National Bureau of Standards, Washington, D.C., 1971.
85. M. HORANI, J. ROSTAS, AND H. LEFEBVRE-BRION, *Canad. J. Phys.* **45,** 3319–3331 (1967).